

Structural identifiability of partially-observed stochastic processes: from single-particle trajectories to total particle density data

Arianna Ceccarelli^{1*}, Alexander P. Browning² and Ruth E. Baker¹

¹Mathematical Institute, University of Oxford, UK.

²School of Mathematics and Statistics, University of Melbourne, Australia.

*Corresponding author. E-mail: ceccarelli@maths.ox.ac.uk;

Abstract

The increasing availability of experimental data has intensified interest in calibrating stochastic models, raising fundamental questions about parameter identifiability. Structural identifiability determines whether parameters can be uniquely recovered from idealised, noise-free data, a prerequisite to allow for parameter estimation. However, existing methods to assess structural identifiability are not generally applicable to stochastic processes. We develop a methodology to analyse structural identifiability for a class of spatio-temporal stochastic processes. We investigate how identifiability depends on the type of available data, distinguishing between single-particle trajectories and total particle density measurements. For trajectory data, we use the individual-based model description that explicitly represents single-particle dynamics. For population-level data, we derive a partial differential equation model representation, that describes the evolution of total particle density, and apply a differential algebra approach, common to ordinary differential equations analysis. We further introduce a novel method to study the initial condition, based on characteristic equations to construct a Taylor expansion of the density evolution, enabling identification of additional identifiable parameter combinations. We apply our methodology to a model, and show it is identifiable with trajectory data but only locally identifiable with density data, and demonstrate the critical role of initial conditions in the identifiability analysis.

Keywords: structural identifiability; stochastic process; hidden Markov model; individual-based model; partial differential equation model; differential algebra; initial condition; Taylor expansion, characteristic equations

1 Introduction

The current growth in the quality and quantity of experimental data collected is leading to an increased interest in calibrating mathematical models to gain quantitative insight. A central question is whether model parameters can be inferred from the available data, referred to as identifiability analysis. When a model is non-identifiable, different parameter combinations can produce indistinguishable model outputs, making model calibration ill-posed. Therefore, identifiability analysis plays a crucial role in determining whether meaningful parameter inference is possible, as well as in guiding model formulation, experimental design, and data collection strategies for complex stochastic systems.

We focus on structural identifiability, which studies whether model parameters can be uniquely determined in an idealised noiseless setting [1–5], in contrast, practical identifiability concerns finite, noisy data [1–3]. Our previous work studies the structural identifiability of stochastic differential equation (SDE) models [6, 7], but there is a lack of general methodologies applicable to study the structural identifiability of stochastic processes. Indeed, it is challenging to link model parameters to observed quantities due to the randomness of these processes. In this work, we propose a novel methodology to study the structural identifiability properties of stochastic processes and how these properties depend on the type of data available, thus determining when reliable parameter inference is possible and what data are required to achieve it.

We consider spatio-temporal stochastic processes that are often captured under either of these two observation regimes, single-particle trajectory data (Figure 1A) and total particle density data (Figure 1B). For partially-observed Markov processes, the challenges in identifying model parameters arise from the data, which may hide the particles’ internal states, complicating the identification of model parameters. Single-particle trajectories are directly obtained from an individual-based description of the continuous-time Markov process, and we provide a method to study the structural identifiability properties measuring these data. We note that from an infinite number of single-particle trajectories, we can extract particle density data by obtaining the distribution of particle locations over time in each different state. However, the converse is

not true; hence, we compare the identifiability properties measuring single-particle trajectories to the total particle density data.

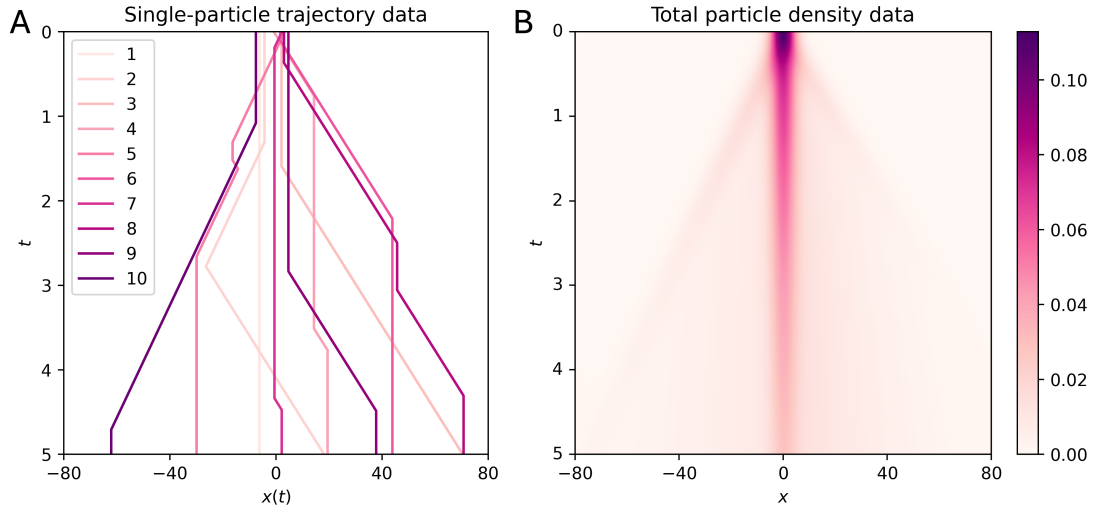


Fig. 1 Comparison of the information obtained from single-particle trajectory data versus total particle density data. The model used to generate the data is described in Section 2. **A** shows examples of single-particle trajectories $x(t)$ numbered 1-10. **B** shows an example of information obtained from total particle density data, $N(x, t)$, which gives no access to the evolution of each particle individually.

For the purpose of structural identifiability, we consider individual tracking data consisting on an infinite number of infinitely-long individual-particle trajectories, which fully capture the location over time t of individual particles (Figure 1A). Moreover, we consider total particle density evolution data, denoted $N(x, t)$, which capture the behaviour of an infinitely-large population of indistinguishable non-interacting particles, in each location x over time t , which partially hides the correlation between the evolution of the location of single particles (Figure 1B). For particle density data, we study the structural identifiability by formulating a differential equation model description of the process describing the density evolution in each state. The methodology presented in this work relies on the availability of a closed-form differential equation description for the particle densities. When such a description cannot be derived, identifiability analysis from density data may require alternative representations, which we do not consider here.

Several methods have been proposed to investigate the structural identifiability of ordinary differential equation (ODE) models [8]; based on differential algebra and differential geometry [9–12], profile likelihoods [13], series expansions [14, 15], or similarity transformations [16]. Moreover, software have been developed to assess the identifiability of ODE models, such as StructuralIdentifiability.jl [17], SIAN [18], GenSSI [19, 20], DAISY [21], STRIKE-GOLDD [22], and StrikePy [23]. The differential algebra approach consists of reducing the system of ODEs through symbolic elimination of unobserved state quantities to *input-output equations* that depend only on the model parameters and on measurable quantities. Two parameter sets are indistinguishable if they generate equivalent input–output equations, and thus identical observable behaviour [5, 12, 14, 24]. The coefficients of the input-output equations, written as model parameter combinations, are analysed to assess whether the model parameters are uniquely determined.

The differential algebra approach has been extended to assess the structural identifiability of partial differential equation (PDE) models [25–28], while alternative approaches study PDE structural identifiability locally using the Fisher information matrix [29, 30]. We apply and extend the differential algebra approach to study the structural identifiability of PDE formulation of the process considered.

The initial conditions are also known to impact the structural identifiability properties of a model as they influence the model solution [12, 31–33], and they have been studied using the differential algebra approach proposed in [27]. However, for some processes, the differential algebra approach alone may not capture all the identifiability information arising from the initial condition. Hence, we propose a novel approach based on writing the model solution close to the initial time as a Taylor series expansion. The coefficients of the Taylor expansions are written in terms of the model and initial condition parameters and may give additional identifiable parameter combinations. We apply this method and highlight how the initial conditions impact the identifiability properties of the model.

In Section 2 we introduce the stochastic process used to showcase our methods, first presented as an individual-based model, which directly describes single-particle trajectories. Moreover, we derive a PDE representation of the stochastic model, which describes the evolution of the particle densities in each state. In Section 3, we analyse the structural identifiability properties of

the model with data consisting of an infinite number of single-particle trajectories. In Section 4, we analyse structural identifiability with data measuring the total particle density, applying the differential algebra approach to the PDE model. Moreover, we propose a new method to study the identifiability properties of the initial conditions and how they impact the identifiability of the model parameters. Finally, in Section 5, we discuss the main contributions of this work, highlighting the differences between the structural identifiability properties of the model with data measuring single-particle trajectories versus total particle density, and we outline potential future directions.

2 The model and its individual-based versus population-level representations

We introduce an example model to showcase the application of the methods we propose for studying the structural identifiability properties of stochastic models, characterised by jumps between states characterised by fixed velocities. Velocity-jump models have been used to describe motion in several contexts, for example, microtubular transport along the axons of neurons [34–41], cell, animal or bacterial motility and chemotaxis [42–45], and swarm robotic motion [46, 47]. However, the structural identifiability properties of these models have not been studied. Hence, we illustrate our methods by applying them to a stochastic velocity-jump model in one spatial dimension, in which the particle’s internal state evolves as a continuous-time Markov chain within a network of three states [48, 49]. We assume that each state is characterised by a constant velocity and fixed rates of switching to every other state; thus, the particle’s state evolution fully characterises its motion [48, 49] (Figure 2A).

2.1 The stochastic individual-based model representation

We first consider the stochastic individual-based version of the model, which directly describes the motion of a single particle in one spatial dimension characterised by three internal states, as described in [48, 49] (Figure 2A). Each state $s = 1, 2, 3$ is associated with a fixed velocity $v_s \in \mathbb{R}$, an exponential state-switching process with rate $\lambda_s > 0$, and fixed transition probabilities to any other state $u \neq s$, denoted $p_{su} \in [0, 1]$, such that $p_{12} + p_{13} = 1$, $p_{21} + p_{23} = 1$, and

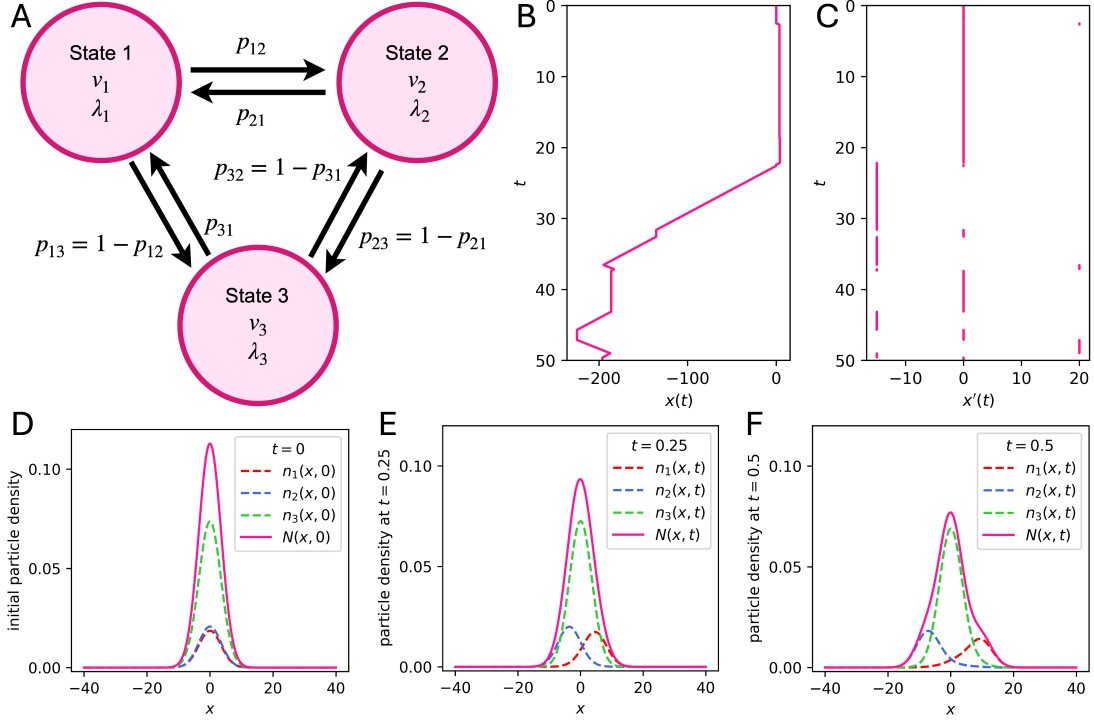


Fig. 2 The model and the two types of data considered to study its structural identifiability. **A** is a graphic visualisation of the three-state individual-based representation. Panels **B-F** are produced using model **A**, with parameter set $\theta_A = \{v_1 = 20, v_2 = -15, v_3 = 0, \lambda_1 = 1, \lambda_2 = 1/2, \lambda_3 = 3/10, p_{12} = 1/5, p_{21} = 3/10, p_{31} = 7/10\}$. **B** shows a portion of an infinite single-particle trajectory $x(t)$ generated using the parametrised model in **A**. **C** shows the piecewise-constant function $x'(t)$, where it exists, obtained from the single-particle trajectory in **B**. **D** shows the initial particle densities in each state at time $t = 0$, $n_s(x, 0) = a_s \exp(-x^2/\zeta^2)/\sqrt{\pi\zeta^2}$, for $s = 1, 2, 3$, with $\zeta = 5$ and $[a_1, a_2, a_3]^T = [237/1441, 24/131, 940/1441]^T$ equal to the stationary distribution (see Supplementary Information Section S1) (dashed lines), and the total density $N(x, 0)$ (continuous line). **E-F** show the evolution of the particle densities in each state (dashed lines) and the total particle density (continuous line) at time $t = 0.25$ and $t = 0.5$, respectively, with initial condition in **D**.

$p_{31} + p_{32} = 1$. These probabilities give the switching probability matrix $\mathbf{P} = [p_{su}]$, defined with zero diagonal entries. Hence, the model considered has a set of nine parameters to identify, $\theta = \{v_1, v_2, v_3, \lambda_1, \lambda_2, \lambda_3, p_{12}, p_{21}, p_{31}\}$ (as $p_{13} = 1 - p_{12}$, $p_{23} = 1 - p_{21}$ and $p_{32} = 1 - p_{31}$; see Figure 2A).

The state evolution is a continuous-time Markov chain, and we define its transition matrix \mathbf{Q} in terms of the total switching rates λ_s and the transition probabilities p_{su} as

$$\mathbf{Q} = [q_{su}] := \begin{bmatrix} -\lambda_1 & \lambda_1 p_{12} & \lambda_1 p_{13} \\ \lambda_2 p_{21} & -\lambda_2 & \lambda_2 p_{23} \\ \lambda_3 p_{31} & \lambda_3 p_{32} & -\lambda_3 \end{bmatrix} = \begin{bmatrix} -\lambda_1 & \lambda_2 p_{21} & \lambda_3 p_{31} \\ \lambda_1 p_{12} & -\lambda_2 & \lambda_3(1 - p_{31}) \\ \lambda_1(1 - p_{12}) & \lambda_2(1 - p_{21}) & -\lambda_3 \end{bmatrix}. \quad (1)$$

Finally, since we assume that the model parameters do not depend on space or time, we may assume that the same applies to the initial condition, which we assume to be separable. We also assume that the particle's initial location is sampled according to a probability distribution function, denoted $f(x)$. Moreover, the particle's initial state is chosen according to a probability vector $\mathbf{a} = [a_1, a_2, a_3]^T$, such that $a_s \in [0, 1]$, for $s = 1, 2, 3$, and $a_1 + a_2 + a_3 = 1$, where a_s is the probability of being in state s at time $t = 0$.

2.2 The population-level system representation

In order to study the structural identifiability of the process parameters, we derive a PDE model that describes the evolution of the particle density in each state s , denoted $n_s(x, t)$, at location x and at time $t \geq 0$, as a Fokker-Planck equation [50]. The three-state reaction-advection PDE model, derived in Supplementary Information Section S2, is given by

$$\frac{\partial n_1}{\partial t} + v_1 \frac{\partial n_1}{\partial x} = -\lambda_1 n_1 + \lambda_2 p_{21} n_2 + \lambda_3 p_{31} n_3, \quad (2a)$$

$$\frac{\partial n_2}{\partial t} + v_2 \frac{\partial n_2}{\partial x} = \lambda_1 p_{12} n_1 - \lambda_2 n_2 + \lambda_3(1 - p_{31}) n_3, \quad (2b)$$

$$\frac{\partial n_3}{\partial t} + v_3 \frac{\partial n_3}{\partial x} = \lambda_1(1 - p_{12}) n_1 + \lambda_2(1 - p_{21}) n_2 - \lambda_3 n_3, \quad (2c)$$

for $t \geq 0$ and $x \in \mathbb{R}$, where $\lambda_s > 0$ for $s \in \{1, 2, 3\}$, and $p_{12}, p_{21}, p_{31} \in [0, 1]$.

In principle, the initial condition in each state could be any analytic function, but in the case of the individual-based model we assumed a separable initial condition and that the model parameters are not spatially-dependent or time-dependent. The particle's initial location is sampled according to a probability distribution function $f(x) \geq 0$, and, in each location, the particles are distributed across states according to the probability vector $\mathbf{a} = [a_1, a_2, a_3]^T$, with

$a_s \in [0, 1]$ and $a_1 + a_2 + a_3 = 1$. Analogously, when measuring the total particle density, we work in the assumption that at the start of the ideal experiment the initial density in each state $s = 1, 2, 3$ is

$$n_s(x, 0) = a_s f(x), \quad (3)$$

where $f(x) = N(x, 0)$ is the initial total particle density. We consider far-field boundary conditions, that are independent of unknown parameters. For simplicity, when generating numerical solutions of the model, we use periodic boundary conditions in the bounded domain $[-L, L]$ with L sufficiently large such that $N(x, t) \approx 0$ in the time interval considered for the simulation with $t \in [0, T]$. This is possible since the initial condition is chosen as a Gaussian around zero, $N(x, 0) = \exp(-x^2/\zeta^2)/\sqrt{\pi\zeta^2}$. We note that equivalent numerical results would be obtained with far-field boundary conditions.

In the examples provided, the numerical simulations of the PDE model solutions are obtained with a first-order upwind scheme for the spatial discretisation, setting the grid to $dx = 0.01$. Then, the time integration is obtained with the automatic method switching discretisation LSODA [51], with output time discretisation with $dt = 0.00045$, which ensures that the Courant–Friedrichs–Lewy stability condition is satisfied [52].

To study the structural identifiability properties of the processes, we assess the uniqueness of the parameters from the observable data, which partially measure the model solution. Hence, we only consider the cases in which the model solution exists and is unique. We note that for any parameter choice, the PDE system has all real eigenvalues v_1, v_2, v_3 , not necessarily distinct, hence, it is *strongly hyperbolic* [53]. Strong hyperbolicity guarantees that solutions to the Cauchy problem (consisting of the PDEs, the initial condition and the boundary conditions) exist, are unique, and depend continuously on the initial data [53].

3 The model parameters are structurally identifiable measuring single-particle trajectories

Now, we propose a novel method to analyse the structural identifiability properties of the individual-based model defined in Section 2, assuming that we measure infinitely a countably

infinite long single-particle trajectories denoted $x_1(t), x_2(t), \dots$ (Figure 1A). We initially consider a single infinitely-long trajectory denoted $x(t)$. For a velocity-jump process, the derivative of a trajectory $x(t)$, $x'(t)$, can be used to obtain the model velocities. Indeed, since the velocity jumps are at discrete times, $x(t)$ is continuous but only piecewise differentiable (Figure 2B). In particular, $x'(t)$ is defined almost everywhere and piecewise constant, and takes values in the set $\{v_1, v_2, v_3\}$ (Figure 2C).

Here, we consider the case in which all velocities are distinct, while the cases in which two or all three velocities are the same are analysed in Supplementary Information Section S3. If all velocities are distinct, the time intervals with constant velocity v_s correspond to the times spent in state s , as the velocity directly identifies the state. The lengths of all time intervals spent in a state s can be obtained and denoted $\tau_s^1, \tau_s^2, \dots$. Then, we can obtain the cumulative distribution of the time spent in each state $s = 1, 2, 3$, as

$$\mathbb{P}(t_s \leq t) = \lim_{K \rightarrow \infty} \frac{1}{K} \sum_{k=1}^K \mathbb{1}(\tau_s^k \leq t),$$

where t_s denotes the time spent in state s before switching and $\mathbb{1}$ is the indicator function. For every state $s = 1, 2, 3$, the cumulative distribution $\mathbb{P}(t_s \leq t) = 1 - \exp(-\lambda_s t)$ is observed, or equivalently, the survival probability $\mathbb{P}(t_s > t) = \exp(-\lambda_s t)$, and it can be used to obtain the switching rate λ_s as

$$\frac{d \exp(-\lambda_s t)}{dt} / \exp(-\lambda_s t) = -\lambda_s.$$

Hence, the switching rates λ_s are also identifiable. Finally, the transition probability from state s to state u can be obtained as

$$p_{su} = \lim_{t \rightarrow \infty} \frac{N_{su}(t)}{N_s(t)},$$

where $N_{su}(t)$ denotes the measured number of switches from state s to u in the time interval $[0, t]$, and $N_s(t)$ denotes the total number of switches from state s to any other state in the time interval $[0, t]$ for the trajectory $x(t)$.

Finally, we analyse the identifiability of the initial condition. From a single trajectory, we can only identify the initial particle's location $x(0)$. In order to identify the initial condition, we need to measure a countably infinite number of trajectories $x_1(t), x_2(t), \dots$. First, we can

obtain the cumulative distribution of the initial location as

$$F(x) = \lim_{M \rightarrow \infty} \frac{1}{M} \sum_{m=1}^M \mathbb{1}(x_m(0) \leq x),$$

and the probability distribution function is obtained as $f(x) = F'(x)$. Moreover, we can obtain the particle's initial state probability vector $\mathbf{a} = [a_1, a_2, a_3]^T$, as the proportion of particles in each state s , with velocity v_s , at time $t = 0$, writing

$$a_s = \lim_{M \rightarrow \infty} \frac{1}{M} \sum_{m=1}^M \mathbb{1}(x'_m(0) = v_s).$$

In summary, all model parameters including the initial condition are, therefore, structurally identifiable, up to state relabelling, using a countably infinite number of single-particle trajectories.

4 Structural identifiability measuring the total particle density can be assessed by formulating a PDE model

In this section, we study the structural identifiability of the parameters of the stochastic process measuring the total particle density. We present a novel method to study the structural identifiability properties of stochastic processes measuring the total particle density evolution, $N(x, t) = n_1(x, t) + n_2(x, t) + n_3(x, t)$ and all its derivatives. In particular, in Section 2.2 we formulated a PDE model that describes the evolution of the particle density in each state, and now we apply the differential algebra approach to the PDE system to obtain identifiable parameter combinations. Then, as the initial condition is known to affect the identifiability properties of PDE systems, we incorporate its study into the analysis by proposing and applying a novel method.

4.1 A first structural identifiability analysis using the differential algebra approach

The differential algebra approach determines structural identifiability by applying differential elimination techniques to remove unobserved state variables from the governing equations. This procedure yields a set of input–output equations that involve only observable quantities and model parameters, and two parameter sets are indistinguishable if they generate identical input–output equations, and thus identical observable behaviour [5, 12, 14, 24]. In other words, the coefficients of the input–output equations, written as parameter combinations, are structurally identifiable.

For linear PDE systems, input–output equations can be obtained by repeatedly differentiating the governing equations and combining them to form a larger PDE system, which can then be solved to eliminate the unobserved variables [27]. Although this procedure is, in principle, systematic and broadly applicable, the number and order of derivatives required typically increase with the number of hidden states. Consequently, the computational complexity to remove unmeasured quantities grows rapidly for systems with multiple unobserved variables, that need to be manually solved. Assuming that only the total particle density $N(x, t)$ is measured, we first perform analytical simplifications to eliminate the variables n_1 and n_2 from the PDE system, and subsequently, we apply the linear elimination procedure only to the remaining hidden variable n_3 .

Firstly, we remove the unobserved variable $n_1 = N - n_2 - n_3$ from Equation (2) to obtain

$$\frac{\partial N}{\partial t} + v_1 \frac{\partial N}{\partial x} + (v_2 - v_1) \frac{\partial n_2}{\partial x} + (v_3 - v_1) \frac{\partial n_3}{\partial x} = 0. \quad (4)$$

We consider the case in which all velocities are equal in Supplementary Information Section S4. Here, we work in the assumption that at least two velocities are distinct, without loss of generality $v_1 \neq v_2, v_3$, and we can fix a state labelling, for example, such that $v_1 > v_2$. Now, we can divide by $v_1 - v_2 \neq 0$ and use Equation (4) to obtain

$$\frac{\partial n_2}{\partial x} = \frac{N^{(0,1)} + v_1 N^{(1,0)} + (v_3 - v_1) \partial_x n_3}{v_1 - v_2}, \quad (5)$$

where we use the notation

$$N^{(i,j)} = \frac{\partial^{i+j}}{\partial^i x \partial^j t} N(x, t).$$

We differentiate Equation (2b) and Equation (2c) with respect to x , and substitute Equation (5) and its derivatives to obtain equations that involve derivatives of n_3 up to order two, and can be used to write a 6×6 linear system in n_3 and its derivatives. The system can be reduced to obtain the input-output equation

$$N^{(0,3)} + c_1 N^{(1,2)} + c_2 N^{(2,1)} + c_3 N^{(3,0)} + c_4 N^{(0,2)} + c_5 N^{(1,1)} + c_6 N^{(2,0)} + c_7 N^{(0,1)} + c_8 N^{(1,0)} = 0,$$

with coefficients

$$\begin{aligned} c_1 &= v_1 + v_2 + v_3, & c_2 &= v_1 v_2 + v_2 v_3 + v_3 v_1, & c_3 &= v_1 v_2 v_3, \\ c_4 &= \lambda_1 + \lambda_2 + \lambda_3, & c_5 &= \lambda_1(v_2 + v_3) + \lambda_2(v_1 + v_3) + \lambda_3(v_1 + v_2), \\ c_6 &= \lambda_1 v_2 v_3 + \lambda_2 v_1 v_3 + \lambda_3 v_1 v_2, & & & & (6) \\ c_7 &= \lambda_2 \lambda_3 (1 - (1 - p_{21})(1 - p_{31})) + \lambda_1 \lambda_3 (1 - (1 - p_{12})p_{31}) + \lambda_1 \lambda_2 (1 - p_{12}p_{21}), \\ c_8 &= \lambda_2 \lambda_3 (1 - (1 - p_{21})(1 - p_{31}))v_1 + \lambda_1 \lambda_3 (1 - (1 - p_{12})p_{31})v_2 + \lambda_1 \lambda_2 (1 - p_{12}p_{21})v_3. \end{aligned}$$

The calculations to reduce the system to the input-output equation are performed using Mathematica (see supplementary material, code). If at least one of the coefficients of the input-output equation is fixed, for example, when the equation is monic, then all its coefficients are structurally identifiable. In this case, all coefficients c_1, \dots, c_8 are identifiable as the equation is monic in $N^{(0,3)}$.

From the first three coefficients, c_1, c_2, c_3 , we obtain a system of three equations of degree three in three unknowns v_1, v_2, v_3 . From c_1 we can write v_3 in terms of v_1 and v_2 as $v_3 = c_1 - v_1 - v_2$, which gives the identifiability of v_3 once v_1 and v_2 are identified. Substituting the expression for v_3 into c_2, c_3 we obtain the conic $c_2 = v_1 v_2 + v_2(c_1 - v_1 - v_2) + (c_1 - v_1 - v_2)v_1$ and the cubic $c_3 = v_1 v_2 (c_1 - v_1 - v_2)$. The possible solutions for v_1, v_2 are obtained from the intersection of the conic and the cubic. By Bézout's theorem, the intersection has six zeros $(v_1, v_2, c_1 - v_1 - v_2)$ counted with multiplicity [54]. By the symmetry of the system, we note

that, since the model parameter values of (v_1, v_2, v_3) must be a solution of the system given by c_1, c_2, c_3 , then any permutation of those is also a solution. Hence, all six solutions of the system are permutations of (v_1, v_2, v_3) . We conclude that all velocities are identifiable up to state relabelling.

Once the state labelling is fixed, the coefficients c_4, c_5, c_6 form a linear system in the switching rates $\lambda_1, \lambda_2, \lambda_3$. The matrix of the system is

$$\begin{bmatrix} 1 & 1 & 1 \\ v_2 + v_3 & v_1 + v_3 & v_1 + v_2 \\ v_2 v_3 & v_1 v_3 & v_1 v_2 \end{bmatrix},$$

which has determinant $(v_1 - v_2)(v_2 - v_3)(v_1 - v_3)$. We consider the case in which two velocities are equal in Supplementary Information Section S4. In the assumption that the velocities are all distinct, the matrix determinant is non-zero, giving a unique solution for the switching rates $\lambda_1, \lambda_2, \lambda_3$, which are therefore identifiable.

The three probability parameters p_{12}, p_{21}, p_{31} appear only in the two quadratic equations given by fixing the coefficients c_7 and c_8 . As these are two equations in three unknowns, then the probability parameters are non-identifiable by the Implicit Function Theorem in [55]. Figure 3 shows the coefficients c_7 and c_8 in terms of the probability parameters p_{12}, p_{21}, p_{31} for an example parametrised model with $\{v_1 = 20, v_2 = -15, v_3 = 0, \lambda_1 = 1, \lambda_2 = 1/2, \lambda_3 = 3/10\}$. We also note that if one of the probability parameters is fixed, for example p_{12} , then the system can be solved to obtain at most two distinct solutions for (p_{21}, p_{31}) .

Finally, we consider separable initial conditions of the form specified in Equation (3). We note that since $a_3 = 1 - a_1 - a_2$ we need to identify only the two parameters a_1 and a_2 . Firstly, we use the differential algebra approach on the PDE system at the initial time $t = 0$. To obtain the input-output equation related to the initial condition, we sum the three equations in Equation (2) at time $t = 0$ and we obtain

$$N^{(0,1)}(x, 0) + c_9 f'(x) = 0, \tag{7}$$

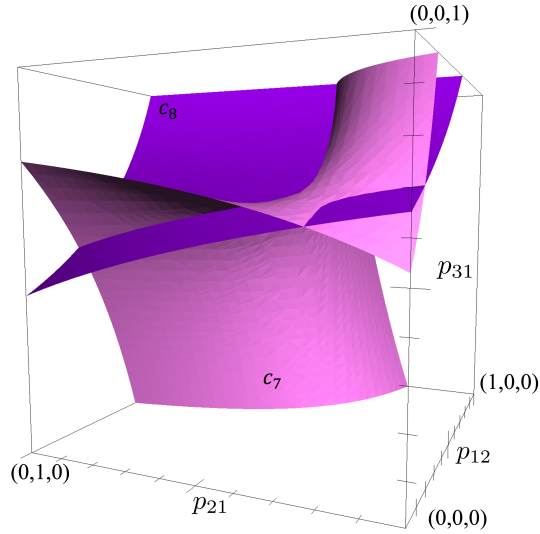


Fig. 3 Example surfaces obtained fixing the coefficients c_7 and c_8 . The surfaces shown are obtained fixing the coefficients $c_7 = 1441/2000$ (pink) and $c_8 = 39/100$ (violet) assuming identified parameters $\theta = \{v_1 = 20, v_2 = -15, v_3 = 0, \lambda_1 = 1, \lambda_2 = 1/2, \lambda_3 = 3/10\}$ and varying $(p_{12}, p_{21}, p_{31}) \in [0, 1] \times [0, 1] \times [0, 1]$. This image was created using Apple Grapher (macOS).

where

$$c_9 = a_1 v_1 + a_2 v_2 + a_3 v_3 = a_1(v_1 - v_3) + a_2(v_2 - v_3) + v_3. \quad (8)$$

Since the coefficients c_1, c_2, c_3 give structural identifiability of the velocities v_1, v_2, v_3 , the coefficient c_9 fixes a line of possible parameters (a_1, a_2) . We conclude that Equation (7) is not sufficient to identify the initial condition and does not add any information to identify the other model parameters.

We note that for some models, the differential algebra approach may be sufficient to find all identifiable parameter combinations that arise from the initial condition [27, 28]. However, as suggested by the numerical examples shown in Supplementary Information Section S5.1, it is not sufficient to study the initial condition for the model we considered. Hence, in the next section, we propose a novel approach to obtain the remaining identifiable coefficients related to the initial condition.

4.2 A novel method based on Taylor expansions of the characteristics to study the initial condition

We consider a Cauchy problem (consisting of the PDE system, the initial condition, and the boundary conditions), and since the PDE system is *strongly hyperbolic*, solutions exist, are unique, and depend continuously on the initial data [53]. First, we obtain the characteristic equations of the PDE system. We rewrite the system in the form

$$\frac{\partial \mathbf{n}}{\partial t} = \mathbf{Q}^T \mathbf{n} - \mathbf{V} \frac{\partial \mathbf{n}}{\partial x}$$

where we write $\mathbf{n} = [n_1(x, t), n_2(x, t), n_3(x, t)]^T$, the diagonal matrix $\mathbf{V} = \text{diag}(v_1, v_2, v_3)$ and \mathbf{Q} is defined in Equation (1). Using the Cauchy-Kovalevskaya theorem [53], we can write the characteristic curves of the PDE system as

$$\frac{dt}{d\tau} v_s = \frac{dx}{d\tau},$$

or equivalently $dx/dt = v_s$, for $s = 1, 2, 3$. On $dx/dt = v_s$, we define $x_s(t) = \xi_s + v_s t$, with initial location $\xi_s = x_s(t=0)$, and $n_s(x_s(0), 0) = n_s(\xi_s, 0) = f_s(\xi_s)$. Then, we write the system characteristic equations as follows

$$\frac{dn_s(x_s(t), t)}{dt} = \sum_{u=1}^3 q_{us} n_u(x_s(t), t), \quad \text{on } x_s(t) = \xi_s + v_s t. \quad (9)$$

Next, we write the Taylor expansion of the density in state s about $t = 0$ as

$$n_s(\xi_s + v_s t, t) = n_s(\xi_s, 0) + \left. \frac{d}{dt} n_s(\xi_s + v_s t, t) \right|_{t=0} t + O(t^2), \quad (10)$$

for every state $s = 1, 2, 3$. Using the initial condition $n_s(x, 0) = a_s f(x)$ and Equation (9), we obtain that, about $t = 0$,

$$n_s(\xi_s + v_s t, t) = a_s f(\xi_s) + t \sum_{u=1}^3 q_{us} a_u f(\xi_s) + O(t^2), \quad (11)$$

for all $\xi_s \in \mathbb{R}$, $s = 1, 2, 3$. We write the Taylor expansion of the total density $N(\xi, t)$ about $t = 0$ at ξ by taking the sum of Equation (11) for $s = 1, 2, 3$, choosing $\xi_s = \xi - v_s t$, as

$$N(\xi, t) = \sum_{s=1}^3 \left(a_s + t \sum_{q=1}^3 q_{us} a_u \right) f(\xi - v_s t) + O(t^2). \quad (12)$$

Finally, Equation (12) can be written as

$$N(\xi, t) = (x_{10} + tc_{13})f(\xi - v_1 t) + (x_{11} + tc_{14})f(\xi - v_2 t) + (x_{12} + tc_{15})f(\xi - v_3 t) + O(t^2),$$

where

$$\begin{aligned} c_{10} &= a_1, & c_{11} &= a_2, & c_{12} &= a_3, \\ c_{13} &= -\lambda_1 a_1 + \lambda_2 p_{21} a_2 + \lambda_3 p_{31} a_3, \\ c_{14} &= \lambda_1 p_{12} a_1 - \lambda_2 a_2 + \lambda_3 (1 - p_{31}) a_3, \\ c_{15} &= \lambda_1 (1 - p_{12}) a_1 + \lambda_2 (1 - p_{21}) a_2 - \lambda_3 a_3. \end{aligned} \quad (13)$$

For a generic initial condition function $f(x)$, in the assumption that the velocities are all distinct, the coefficients $c_{10}, c_{11}, \dots, c_{15}$ are structurally identifiable (see Supplementary Information Section S6 for a proof). The cases in which the velocities are not all distinct are considered in Supplementary Information Section S7.

We note that simply using the differential algebra approach, used in Section 4.1, does not capture all the information related to the initial condition. Indeed, the derivatives of N at $t = 0$ in space and time are directly proportional according to Equation (7), therefore, taking their sum leads to a simplified input-output equation with only the identifiable coefficient c_9 . However, for a generic function $f(x)$ (not constant), $N(x, t)$ shows independent behaviours about $t = 0$ in different locations. The uniqueness of the Taylor expansion of $n_s(x, t)$ allows us to write the model solution in each state about $t = 0$ and, considering their sum, we find additional identifiable parameter combinations, shown in Equation (13).

In Section 4.1, we obtained that after fixing a state labelling, from the coefficients c_1, \dots, c_6 , the velocities v_1, v_2, v_3 and switching rates $\lambda_1, \lambda_2, \lambda_3$ are structurally identifiable. In addition, the coefficients c_{10}, c_{11}, c_{12} allow us to identify a_1, a_2 and $a_3 = 1 - a_1 - a_2$, making the coefficient

c_9 redundant. We also note that $c_{15} = -c_{13} - c_{14}$, making c_{15} also redundant. Hence, we are left with the analysis of the coefficients c_7, c_8, c_{13}, c_{14} to identify the probability parameters p_{12}, p_{21}, p_{31} . The coefficients c_{13}, c_{14} give two planes that are linear in p_{12}, p_{21}, p_{31} , therefore, their intersection gives a line of probability parameters. Then, the parameters p_{12}, p_{21}, p_{31} must lie in the intersection between the line from the intersection between the planes c_{13} and c_{14} (for example, Figure 4A, green line) and the conic and cubic surfaces c_7, c_8 (for example, Figure 4A, pink and purple surfaces).

We conclude that the model is locally structurally identifiable from the parameter combinations c_1, \dots, c_{15} (see the supplementary material, Mathematica code to test equivalence between other model parametrisations). In particular, all parameters are globally structurally identifiable except the three probability parameters which are always at least locally identifiable. In other words, model parameters are uniquely identifiable in a small neighbourhood of the true parameter values. Moreover, we argue that these coefficients c_1, \dots, c_{15} give all the identifiable parameter combinations. Indeed, Figure 4B-C show numerically that the parametrised models A and B, with different probability parameters p_{12}, p_{21}, p_{31} , have identical total particle density evolutions, suggesting there are no additional coefficients to consider. In Supplementary Information Section S5.2 we show that if the initial condition parameters are changed, other equivalent model parameters may exist.

In Section 3, we found that the model parameters are structurally identifiable measuring single-particle trajectories, while we find that they are only locally identifiable measuring the total particle density evolution. Hence, single-particle trajectory and total particle density data lead to different structural identifiability properties.

5 Discussion and conclusions

In this paper, we developed a general methodology to analyse the structural identifiability of spatio-temporal stochastic processes, for which no broadly applicable techniques currently exist. We first introduced a method to study the identifiability properties of partially-observed Markov models measuring single-particle trajectory data. Moreover, we investigated the structural identifiability of stochastic models from measurements of the total particle density by formulating a

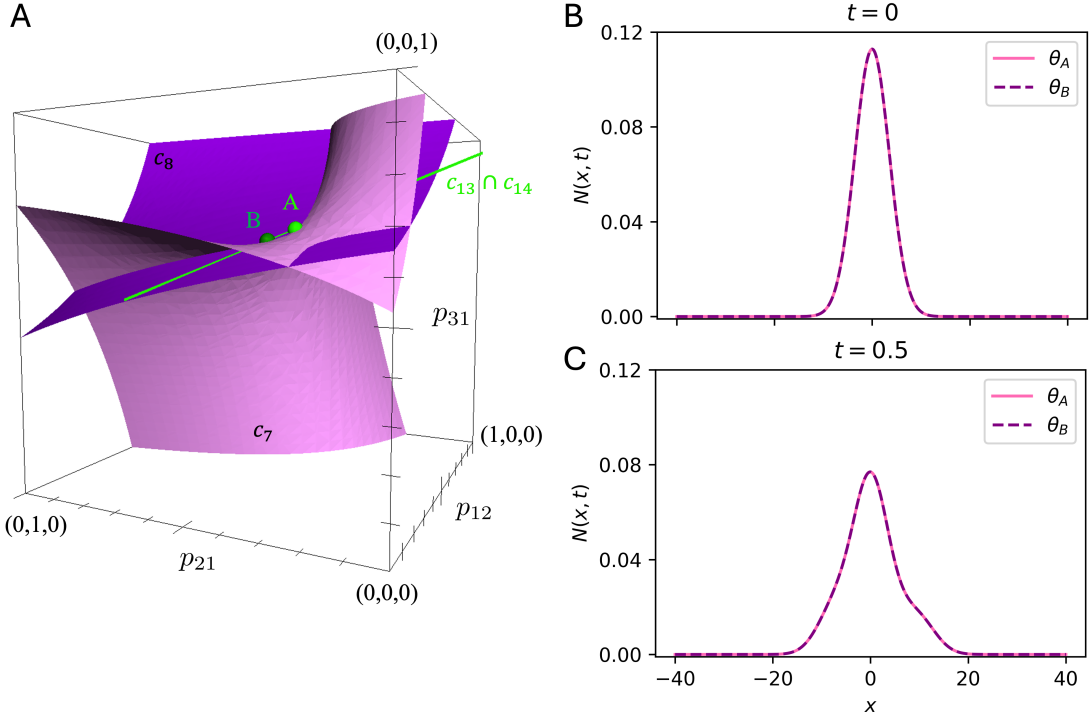


Fig. 4 Local identifiability of the probability parameters leads to structurally identical models A and B and comparison of their numerical solutions at times $t = 0$ and $t = 0.5$. A shows the intersection between the surfaces given by coefficients c_7, c_8 and the line obtained by intersecting c_{13} and c_{14} (green line), using parametrised model A, with parameter set $\{v_1 = 20, v_2 = -15, v_3 = 0, \lambda_1 = 1, \lambda_2 = 1/2, \lambda_3 = 3/10, p_{12} = 1/5, p_{21} = 3/10, p_{31} = 7/10\}$ and initial condition parameters $\{a_1 = 237/1441, a_2 = 24/131, a_3 = 940/1441\}$. The four coefficients intersect in the point $A = \{p_{12} = 1/5, p_{21} = 3/10, p_{31} = 7/10\}$ and in the point $B = \{p_{12} = 66/395, p_{21} = 79/220, p_{31} = 158/235\}$, which denotes model B. This image was created using Apple Grapher (macOS). B-C show the numerical solution for the parametrised model A with the one for model B at times $t = 0$ and $t = 0.5$, respectively.

PDE description. We then applied the differential algebra approach to reduce the PDE system to input-output equations whose coefficients determine the set of identifiable parameter combinations. Finally, we demonstrate that the information given by the initial condition should be incorporated in the structural identifiability analysis, as it is known to have an impact on model identifiability [12, 14, 31–33].

The problem of how to incorporate the initial condition when studying the structural identifiability of PDE models is an open question, which has been partially addressed by evaluating the PDEs at the initial time $t = 0$ and applying the differential algebra approach [27, 28]. However, we found that the differential algebra approach alone is insufficient to analyse the initial condition of the PDE model considered, since the input-output equations at $t = 0$ partially hide

information, which may happen, for example, when the derivatives in space and time of the total density at the initial time are directly proportional (Equation (7)). In Section 4.2, we proposed a novel method to analyse the initial condition based on writing the Taylor expansion of the total particle density about $t = 0$. Particularly, since we measure the total particle density about $t = 0$ in different locations, the Taylor expansion, obtained by using the characteristic equations of the PDE system, gives an additional set of identifiable parameter combinations.

We showcased our methodology by applying it to the model in Section 2, in which the particle’s motion is determined by its hidden internal state, which evolves within a network of three states, with each state characterised by a constant velocity and constant switching rates. Since the model parameters are assumed to be constant in space and time, we also assumed the initial condition the particles in each state to be proportional in space. We obtained that the model parameters are structurally identifiable using single-particle trajectory data but are only locally identifiable using total density measurements.

We also obtained that structurally identical model parameters vary with the initial condition parameters. In particular, we found that the parameter equivalences arising under a certain initial condition may not hold under alternative initial conditions, for example, θ_A and θ_B in Figure 4 are only structurally equivalent under a specific initial condition. This emphasises the link between experimental design and identifiability analysis, as varying the initial condition could be used as a practical strategy to improve parameter identifiability.

We highlight that the structural identifiability measuring single-particle trajectories and the local identifiability measuring the total particle density are valid when the model velocities are all distinct. We note that, if multiple states share precisely the same velocity, single-particle trajectory data are not sufficient to reveal the internal state. The identifiability of Markov models in which different states share similar properties is an area of current research [56]. In Supplementary Information Section S3, we provide a novel method in which we propose to use the waiting time distribution in states with the same velocity, which can be computed using recurrence relations as the particle’s velocity is observable, and we study its identifiability properties. Moreover, in Supplementary Information Sections S4 and S7, we show that if two states share the same velocity, measuring the total particle density leads to parameter non-identifiability. Finally, if all three states share the same velocity, measuring either type of data

leads to the same identifiability results, giving that only the velocity is identifiable, but all other parameters are non-identifiable.

Several avenues for future work emerge from this study. We applied the methods to a three-state model, but the same methods are applicable to obtain information on the identifiability properties of these models with any number of states n , as specified in [48, 49]. The identifiability results measuring single-particle trajectories directly apply to the model with any number of states. For the total particle density data, although the methodology can be applied directly to n -state velocity-jump models, we expect the complexity of the calculations to rapidly increase with the number of states. Moreover, other classes of initial conditions and boundary conditions could be incorporated into the study.

More generally, the proposed methodology could be used to study the structural identifiability measuring particle density data for a class of stochastic models with a differential equation model formulation. The methods proposed to study initial conditions and their identifiability are also applicable to other models for which characteristic equations can be written in terms of the model parameters. For PDE models involving higher order derivatives, further identifiable parameter combinations could appear from orders higher than one in the Taylor expansion method to study the initial condition.

In some biological systems, experimental techniques can detect only stationary or slow-moving particles [57]. Therefore, idealised data could be assumed to only capture particles in a state with zero velocity. The methods are also applicable in the case in which, instead of measuring the total particle density, the data only capture particle density in specific states, but it is unclear whether the identifiability properties would remain the same, especially as the number of states and model complexity increases.

Overall, this work proposes novel methods to analyse the structural identifiability properties of the parameters of a class of stochastic models and highlights how they depend on the nature of the data, capturing either individual behaviour or particle density evolution. From a modelling perspective, these two types of data lead to two natural mathematical representations: individual-based models and differential equation models. This distinction parallels the classical relationship between the Kurtz's random time-change representation and the chemical master

equation, which governs the evolution of the probability densities of the same reaction network [58, 59]. Hence, future work may be done to extend the methodology to chemical reaction models, particularly with relevant spatial components.

Our results characterise parameter identifiability in idealised settings, but real data are finite, noisy, and often partially observed. Therefore, extensions may focus on whether the parameters can be estimated in practice [2, 3]. This motivates future work to analyse the practical identifiability properties of the model considered. More broadly, this work highlights that inference strategies should be tailored to the type of observations available, anticipating potential calibration issues arising from the lack of structural identifiability, as shown in [48].

Declarations

Funding A.C. is supported by a Mathematical Institute Studentship from the University of Oxford. R.E.B. is supported by a grant from the Simons Foundation (MP-SIP-00001828). For the purpose of open access, the author has applied a CC BY public copyright licence to any author accepted manuscript arising from this submission.

Conflict of interest The authors declare that they have no conflict of interest.

Consent for publication All the authors approved the final version of the manuscript.

Code availability The Python files, Mathematica notebook and Apple Grapher files are available on GitHub in the repository

[a-ceccarelli/structural_identifiability_stochastic_processes](https://github.com/a-ceccarelli/structural_identifiability_stochastic_processes).

CRedit author statement A.C.: Writing - Original Draft, Writing - Review and Editing, Conceptualisation, Methodology, Formal Analysis, Visualisation, Software Implementation. A.P.B. and R.E.B.: Supervision, Conceptualisation, Writing - Review and Editing.

References

- [1] Preston, S.P., Wilkinson, R.D., Clayton, R.H., Chappell, M.J., Mirams, G.R.: Think before you fit: Parameter identifiability, sensitivity and uncertainty in systems biology models. *Current Opinion in Systems Biology*, 100563 (2025) <https://doi.org/10.1016/j.coisb.2025.100563>

- [2] Wieland, F.-G., Hauber, A.L., Rosenblatt, M., Tönsing, C., Timmer, J.: On structural and practical identifiability. *Current Opinion in Systems Biology* **25**, 60–69 (2021) <https://doi.org/10.1016/j.coisb.2021.03.005>
- [3] Walter, E.: *Identifiability of Parametric Models*. Elsevier, Amsterdam (2014)
- [4] Cobelli, C., Distefano 3rd, J.J.: Parameter and structural identifiability concepts and ambiguities: a critical review and analysis. *American Journal of Physiology-Regulatory, Integrative and Comparative Physiology* **239**(1), 7–24 (1980) <https://doi.org/10.1152/ajpregu.1980.239.1.R7>
- [5] Bellman, R., Åström, K.J.: On structural identifiability. *Mathematical Biosciences* **7**(3-4), 329–339 (1970) [https://doi.org/10.1016/0025-5564\(70\)90132-X](https://doi.org/10.1016/0025-5564(70)90132-X)
- [6] Browning, A.P., Chappell, M.J., Rahkooy, H., Loman, T.E., Baker, R.E.: Exact identifiability analysis for a class of partially observed near-linear stochastic differential equation models. arXiv preprint arXiv:2503.19241 (2025) <https://doi.org/10.48550/arXiv.2503.19241>
- [7] Browning, A.P., Warne, D.J., Burrage, K., Baker, R.E., Simpson, M.J.: Identifiability analysis for stochastic differential equation models in systems biology. *Journal of the Royal Society Interface* **17**(173), 20200652 (2020) <https://doi.org/10.1098/rsif.2020.0652>
- [8] Miao, H., Xia, X., Perelson, A.S., Wu, H.: On identifiability of nonlinear ODE models and applications in viral dynamics. *SIAM review* **53**(1), 3–39 (2011) <https://doi.org/10.1137/090757009>
- [9] Villaverde, A.F., Barreiro, A., Papachristodoulou, A.: Structural identifiability of dynamic systems biology models. *PLoS Computational Biology* **12**(10), 1005153 (2016) <https://doi.org/10.1098/rsif.2019.0043>
- [10] Raue, A., Karlsson, J., Saccomani, M.P., Jirstrand, M., Timmer, J.: Comparison of approaches for parameter identifiability analysis of biological systems. *Bioinformatics* **30**(10), 1440–1448 (2014) <https://doi.org/10.1093/bioinformatics/btu006>
- [11] Meshkat, N., Eisenberg, M., DiStefano III, J.J.: An algorithm for finding globally identifiable parameter combinations of nonlinear ODE models using Gröbner bases. *Mathematical Biosciences* **222**(2), 61–72 (2009) <https://doi.org/10.1016/j.mbs.2009.08.010>
- [12] Ljung, L., Glad, T.: On global identifiability for arbitrary model parametrizations. *Automatica* **30**(2), 265–276 (1994) [https://doi.org/10.1016/0005-1098\(94\)90029-9](https://doi.org/10.1016/0005-1098(94)90029-9)
- [13] Raue, A., Kreutz, C., Maiwald, T., Bachmann, J., Schilling, M., Klingmüller, U., Timmer, J.: Structural and practical identifiability analysis of partially observed dynamical models by exploiting the profile likelihood. *Bioinformatics* **25**(15), 1923–1929 (2009) <https://doi.org/10.1093/bioinformatics/btp358>
- [14] Saccomani, M.P., Audoly, S., D’Angiò, L.: Parameter identifiability of nonlinear systems: the role of initial conditions. *Automatica* **39**(4), 619–632 (2003) [https://doi.org/10.1016/S0005-1098\(02\)00302-3](https://doi.org/10.1016/S0005-1098(02)00302-3)

- [15] Pohjanpalo, H.: System identifiability based on the power series expansion of the solution. *Mathematical Biosciences* **41**(1-2), 21–33 (1978) [https://doi.org/10.1016/0025-5564\(78\)90063-9](https://doi.org/10.1016/0025-5564(78)90063-9)
- [16] Vajda, S., Godfrey, K.R., Rabitz, H.: Similarity transformation approach to identifiability analysis of nonlinear compartmental models. *Mathematical Biosciences* **93**(2), 217–248 (1989) [https://doi.org/10.1016/0025-5564\(89\)90024-2](https://doi.org/10.1016/0025-5564(89)90024-2)
- [17] Dong, R., Goodbrake, C., Harrington, H., Pogudin, G.: Differential elimination for dynamical models via projections with applications to structural identifiability. *SIAM Journal on Applied Algebra and Geometry* **7**(1), 194–235 (2023) <https://doi.org/10.1137/22M1469067>
- [18] Hong, H., Ovchinnikov, A., Pogudin, G., Yap, C.: SIAN: software for structural identifiability analysis of ODE models. *Bioinformatics* **35**(16), 2873–2874 (2019) <https://doi.org/10.1093/bioinformatics/bty1069>
- [19] Ligon, T.S., Fröhlich, F., Chiş, O.T., Banga, J.R., Balsa-Canto, E., Hasenauer, J.: GenSSI 2.0: multi-experiment structural identifiability analysis of SBML models. *Bioinformatics* **34**(8), 1421–1423 (2018) <https://doi.org/10.1093/bioinformatics/btx735>
- [20] Chiş, O., Banga, J.R., Balsa-Canto, E.: GenSSI: a software toolbox for structural identifiability analysis of biological models. *Bioinformatics* **27**(18), 2610–2611 (2011) <https://doi.org/10.1093/bioinformatics/btr431>
- [21] Bellu, G., Saccomani, M.P., Audoly, S., D’Angiò, L.: DAISY: A new software tool to test global identifiability of biological and physiological systems. *Computer Methods and Programs in Biomedicine* **88**(1), 52–61 (2007) <https://doi.org/10.1016/j.cmpb.2007.07.002>
- [22] Díaz-Seoane, S., Rey Barreiro, X., Villaverde, A.F.: STRIKE-GOLDD 4.0: user-friendly, efficient analysis of structural identifiability and observability. *Bioinformatics* **39**(1), 748 (2023) <https://doi.org/10.1093/bioinformatics/btac748>
- [23] Rey Rostro, D., Villaverde, A.: StrikePy: Nonlinear observability analysis of inputs, states, and parameters in Python. *XLIII Jornadas de Automática: libro de actas*, 430–435 (2022) <https://doi.org/10.17979/spudc.9788497498418.0430>
- [24] Audoly, S., Bellu, G., D’Angio, L., Saccomani, M.P., Cobelli, C.: Global identifiability of nonlinear models of biological systems. *IEEE Transactions on Biomedical Engineering* **48**(1), 55–65 (2002) <https://doi.org/10.1109/10.900248>
- [25] Byrne, H.M., Harrington, H.A., Ovchinnikov, A., Pogudin, G., Rahkooy, H., Soto, P.: Algebraic identifiability of partial differential equation models. *Nonlinearity* **38**(2), 025022 (2025) <https://doi.org/10.1088/1361-6544/ada510>
- [26] Salmaniw, Y., Browning, A.P.: Structural identifiability of linear-in-parameter parabolic PDEs through auxiliary elliptic operators. *Journal of Mathematical Biology* **91**(1), 4 (2025) <https://doi.org/10.1007/s00285-025-02225-w>
- [27] Browning, A.P., Taşcă, M., Falcó, C., Baker, R.E.: Structural identifiability analysis of linear reaction–advection–diffusion processes in mathematical biology. *Proceedings of the Royal Society A* **480**(2286), 20230911 (2024) <https://doi.org/10.1098/rspa.2023.0911>

- [28] Renardy, M., Kirschner, D., Eisenberg, M.: Structural identifiability analysis of age-structured PDE epidemic models. *Journal of Mathematical Biology* **84**(1), 9 (2022) <https://doi.org/10.1007/s00285-021-01711-1>
- [29] Ciocanel, M.-V., Ding, L., Mastromatteo, L., Reichheld, S., Cabral, S., Mowry, K., Sandstede, B.: Parameter identifiability in PDE models of fluorescence recovery after photobleaching. *Bulletin of Mathematical Biology* **86**(4), 36 (2024) <https://doi.org/10.1007/s11538-024-01266-4>
- [30] Eisenberg, M.C., Hayashi, M.A.: Determining identifiable parameter combinations using subset profiling. *Mathematical Biosciences* **256**, 116–126 (2014) <https://doi.org/10.1016/j.mbs.2014.08.008>
- [31] Chis, O.-T., Banga, J.R., Balsa-Canto, E.: Structural identifiability of systems biology models: a critical comparison of methods. *PloS One* **6**(11), 27755 (2011) <https://doi.org/10.1371/journal.pone.0027755>
- [32] Diop, S., Fliess, M.: Nonlinear observability, identifiability, and persistent trajectories. In: [1991] *Proceedings of the 30th IEEE Conference on Decision and Control*, pp. 714–719 (1991). <https://doi.org/10.1109/CDC.1991.261405>
- [33] Tunali, E., Tarn, T.-J.: New results for identifiability of nonlinear systems. *IEEE Transactions on Automatic Control* **32**(2), 146–154 (1987) <https://doi.org/10.1109/TAC.1987.1104544>
- [34] Bressloff, P.C.: Queuing model of axonal transport. *Brain Multiphysics* **2**, 100042 (2021) <https://doi.org/10.1016/j.brain.2021.100042>
- [35] Xue, C., Jameson, G.: Recent mathematical models of axonal transport. *Stochastic Processes, Multiscale Modeling, and Numerical Methods for Computational Cellular Biology*, 265–285 (2017) https://doi.org/10.1007/978-3-319-62627-7_12
- [36] Encalada, S.E., Goldstein, L.S.: Biophysical challenges to axonal transport: motor-cargo deficiencies and neurodegeneration. *Annual Review of Biophysics* **43**, 141–169 (2014) <https://doi.org/10.1146/annurev-biophys-051013-022746>
- [37] Bressloff, P.C., Newby, J.M.: Stochastic models of intracellular transport. *Reviews of Modern Physics* **85**(1), 135–196 (2013) <https://doi.org/10.1103/RevModPhys.85.135>
- [38] Kuznetsov, A.V.: Analytical solution of equations describing slow axonal transport based on the stop-and-go hypothesis. *Central European Journal of Physics* **9**(3), 662–673 (2011) <https://doi.org/10.2478/s11534-010-0066-0>
- [39] Jung, P., Brown, A.: Modeling the slowing of neurofilament transport along the mouse sciatic nerve. *Physical Biology* **6**(4), 046002 (2009) <https://doi.org/10.1088/1478-3975/6/4/046002>
- [40] Friedman, A., Craciun, G.: A model of intracellular transport of particles in an axon. *Journal of Mathematical Biology* **51**(2), 217–246 (2005) <https://doi.org/10.1007/s00285-004-0285-3>

- [41] Brown, A.: Slow axonal transport: stop and go traffic in the axon. *Nature Reviews Molecular Cell Biology* **1**(2), 153–156 (2000) <https://doi.org/10.1038/35040102>
- [42] Taylor-King, J.P., Loon, E.E., Rosser, G., Chapman, S.J.: From birds to bacteria: generalised velocity jump processes with resting states. *Bulletin of Mathematical Biology* **77**, 1213–1236 (2015) <https://doi.org/10.1007/s11538-015-0083-7>
- [43] Treloar, K.K., Simpson, M.J., McCue, S.W.: Velocity-jump models with crowding effects. *Physical Review E—Statistical, Nonlinear, and Soft Matter Physics* **84**(6), 061920 (2011) <https://doi.org/10.1103/PhysRevE.84.061920>
- [44] Erban, R., Othmer, H.G.: From individual to collective behavior in bacterial chemotaxis. *SIAM Journal on Applied Mathematics* **65**(2), 361–391 (2004) <https://doi.org/10.1137/S0036139903433232>
- [45] Othmer, H.G., Dunbar, S.R., Alt, W.: Models of dispersal in biological systems. *Journal of Mathematical Biology* **26**(3), 263–298 (1988) <https://doi.org/10.1007/BF00277392>
- [46] Franz, B., Taylor-King, J.P., Yates, C., Erban, R.: Hard-sphere interactions in velocity-jump models. *Physical Review E* **94**(1), 012129 (2016) <https://doi.org/10.1103/PhysRevE.94.012129>
- [47] Taylor-King, J.P., Franz, B., Yates, C.A., Erban, R.: Mathematical modelling of turning delays in swarm robotics. *IMA Journal of Applied Mathematics* **80**(5), 1454–1474 (2015) <https://doi.org/10.1093/imamat/hxv001>
- [48] Ceccarelli, A., Browning, A.P., Chaiamarit, T., Davis, I., Baker, R.E.: A likelihood-based Bayesian inference framework for the calibration of and selection between stochastic velocity-jump models. *Journal of the Royal Society Interface* **23**(236), 20250866 (2026) <https://doi.org/10.1098/rsif.2025.0866>
- [49] Ceccarelli, A., Browning, A.P., Baker, R.E.: Approximate solutions of a general stochastic velocity-jump model subject to discrete-time noisy observations. *Bulletin of Mathematical Biology* **87**(57) (2025) <https://doi.org/10.1007/s11538-025-01437-x>
- [50] Gardiner, C.: Markov processes. In: *Elements of Stochastic Methods*, pp. 42–76. AIP Publishing LLC, Melville, New York (2009). https://doi.org/10.1063/9780735423718_004
- [51] Petzold, L.: Automatic selection of methods for solving stiff and nonstiff systems of ordinary differential equations. *SIAM Journal on Scientific and Statistical Computing* **4**(1), 136–148 (1983) <https://doi.org/10.1137/0904010>
- [52] Courant, R., Friedrichs, K., Lewy, H.: On the partial difference equations of mathematical physics. *IBM Journal of Research and Development* **11**(2), 215–234 (1967) <https://doi.org/10.1147/rd.112.0215>
- [53] Godlewski, E., Raviart, P.-A.: *Hyperbolic Systems of Conservation Laws vol. 3-4*. Ellipses, Paris (1991)
- [54] Fulton, W.: *Algebraic Curves: An Introduction to Algebraic Geometry*. Addison Wesley Longman Publishing Co, Reading, Massachusetts (1969)

- [55] Rudin, W.: Principles of Mathematical Analysis. McGraw-Hill, New York (1976)
- [56] Siekmann, I.: Modelling ion channels with a view towards identifiability. *Bulletin of Mathematical Biology* **88**(1), 2 (2026) <https://doi.org/10.1007/s11538-025-01558-3>
- [57] Syga, Ł., Spakman, D., Punter, C.M., Poolman, B.: Method for immobilization of living and synthetic cells for high-resolution imaging and single-particle tracking. *Scientific Reports* **8**(1), 13789 (2018) <https://doi.org/10.1038/s41598-018-32166-y>
- [58] Anderson, D.F., Kurtz, T.G., Koeppl, H., Setti, G., Bernardo, M., Densmore, D.: Continuous time Markov chain models for chemical reaction networks. In: *Design and Analysis of Biomolecular Circuits: Engineering Approaches to Systems and Synthetic Biology*, pp. 3–42. Springer, New York (2011). https://doi.org/10.1007/978-1-4419-6766-4_1
- [59] Kurtz, T.G.: Representations of Markov processes as multiparameter time changes. *The Annals of Probability*, 682–715 (1980)

Supplementary Information

Structural identifiability of partially-observed
stochastic processes: from single-particle
trajectories to total particle density data

Arianna Ceccarelli^{1*}, Alexander P. Browning² and Ruth E. Baker¹

¹Mathematical Institute, University of Oxford, UK.

²School of Mathematics and Statistics, University of Melbourne, Australia.

*Corresponding author. E-mail: ceccarelli@maths.ox.ac.uk;

Contents

S1 The stochastic model stationary distribution	2
S2 The PDE system derivation from the individual-based model	2
S3 Structural identifiability measuring single-particle trajectories if two or three states share the same velocity	5
S4 Structural identifiability measuring the total particle density if two or three states share the same velocity	10
S5 Examples of equivalent model parametrisations and the impact of the initial condition with velocities all distinct	11
S5.1 Fixing the coefficients c_1, \dots, c_9 is not sufficient to obtain identical total density evolutions	13
S5.2 The coefficients c_1, \dots, c_{15} give local structural identifiability	16

S6 There exist three linearly independent vectors of the type $F_z(t)$ if all three velocities are distinct 17

S7 Structural identifiability measuring the total particle density if two or three states share the same velocity incorporating the initial condition 18

S1 The stochastic model stationary distribution

The stationary distribution of a continuous-time Markov chain should be studied as it describes the system's long-run behaviour and it can be used to identify the model parameters that relate to its transition matrix \mathbf{Q} . We note that, under the assumption of the state continuous-time Markov chain being irreducible, the stochastic model transition matrix \mathbf{Q} has a unique stationary distribution (see [1, 2]). If $\boldsymbol{\pi} = [\pi_1, \pi_2, \pi_3]^T$ is any eigenvector in the kernel of \mathbf{Q}^T , such that $\mathbf{Q}^T \boldsymbol{\pi} = \mathbf{0}$, then the stationary distribution $\boldsymbol{w} = [w_1, w_2, w_3]^T$ is the unique solution of the system $\mathbf{Q}^T \boldsymbol{w} = \mathbf{0}$ with $w_s \geq 0$ for $s = 1, 2, 3$ and $w_3 = 1 - w_1 - w_2$, obtained as $\boldsymbol{w} = \boldsymbol{\pi} / (\pi_1 + \pi_2 + \pi_3)$.

The stationary distribution \boldsymbol{w} is unique and it can be written in terms of the switching rates and probability parameters as

$$\boldsymbol{w} = \frac{[\phi_1, \phi_2, \phi_3]^T}{\phi_1 + \phi_2 + \phi_3}, \quad \text{with } \phi_s = \lambda_u \lambda_z (1 - p_{uz} p_{zu}), \quad (\text{S1})$$

for $(s, z, u) \in \{(1, 2, 3), (2, 1, 3), (3, 1, 2)\}$. Equivalently, we write the stationary distribution in terms of the switching rates and the probability parameters p_{12}, p_{21}, p_{31} as

$$\begin{aligned} w_1 &= \frac{\lambda_2 \lambda_3 (1 - (1 - p_{21})(1 - p_{31}))}{\lambda_2 \lambda_3 (1 - (1 - p_{21})(1 - p_{31})) + \lambda_1 \lambda_3 (1 - (1 - p_{12})p_{31}) + \lambda_1 \lambda_2 (1 - p_{12}p_{21})}, \\ w_2 &= \frac{\lambda_1 \lambda_3 (1 - (1 - p_{12})p_{31})}{\lambda_2 \lambda_3 (1 - (1 - p_{21})(1 - p_{31})) + \lambda_1 \lambda_3 (1 - (1 - p_{12})p_{31}) + \lambda_1 \lambda_2 (1 - p_{12}p_{21})}, \\ w_3 &= \frac{\lambda_1 \lambda_2 (1 - p_{12}p_{21})}{\lambda_2 \lambda_3 (1 - (1 - p_{21})(1 - p_{31})) + \lambda_1 \lambda_3 (1 - (1 - p_{12})p_{31}) + \lambda_1 \lambda_2 (1 - p_{12}p_{21})}. \end{aligned} \quad (\text{S2})$$

S2 The PDE system derivation from the individual-based model

In this section, we derive the PDE system describing the evolution of the particle density in each state $s = 1, 2, 3$ at location x and at time t , $n_s(x, t)$, as a Fokker-Planck equation.

We fix a small time increment Δt , and denote the density in state s , at location x and time $t + \Delta t$, $n_s(x, t + \Delta t)$ which we write as a sum of terms up to order $o(\Delta t)$. The first term is the density of particles in state s at time t , at the location $x - v_s \Delta t$ that remain in state s , which can be written as $(1 - \lambda_s \Delta t) n_s(x - v_s \Delta t, t)$. Then, we add, for each state $u \neq s$, the density of particles at state u , that switch state exactly once, to state s , at time $t + \hat{\Delta} t \in [t, t + \Delta t)$, with $0 \leq \hat{\Delta} t < \Delta t$, which at time t is at location $x - v_u \hat{\Delta} t - v_s(\Delta t - \hat{\Delta} t)$, and can be written as $(\lambda_u p_{us} \Delta t) n_u(x - v_u \hat{\Delta} t - v_s(\Delta t - \hat{\Delta} t), t)$. Hence, we obtain

$$n_s(x, t + \Delta t) = (1 - \lambda_s \Delta t) n_s(x - v_s \Delta t, t) + \sum_{u \neq s} (\lambda_u p_{us} \Delta t) n_u(x - v_u \hat{\Delta} t - v_s(\Delta t - \hat{\Delta} t), t) + o(\Delta t),$$

which, expanding the terms to the first order in Δt , gives

$$\begin{aligned} n_s(x, t) + (\Delta t) \partial_t n_s(x, t) &= (1 - \lambda_s \Delta t) (n_s(x, t) - (v_s \Delta t) \partial_x n_s(x, t) + o(\Delta t)) \\ &\quad + \sum_{u \neq s} (\lambda_u p_{us} \Delta t) (n_u(x, t) - (v_s \Delta t + (v_u - v_s) \hat{\Delta} t) \partial_x n_u(x, t) + o(\Delta t)) \\ &\quad + o(\Delta t). \end{aligned}$$

By simplifying, rearranging, using $\hat{\Delta} t < \Delta t$, and grouping the terms of order higher than one in Δt in $o(\Delta t)$, we obtain

$$(\Delta t) \partial_t n_s = -(v_s \Delta t) \partial_x n_s(x, t) + (-\lambda_s \Delta t) n_s(x, t) + \sum_{u \neq s} (\lambda_u p_{us} \Delta t) (n_u(x, t)) + o(\Delta t)$$

and to conclude we divide by Δt and let $\Delta t \rightarrow 0$.

We obtain the three-state reaction-advection PDE model, that describes the evolution of the particle density in state $s = 1, 2, 3$ at location x and at time t , $n_s(x, t)$, as

$$\frac{\partial n_s(x, t)}{\partial t} + v_s \frac{\partial n_s(x, t)}{\partial x} = \sum_{u=1}^3 q_{us} n_u(x, t). \quad (\text{S3})$$

In this work, we assume that we can measure only the total density

$$N(x, t) = \sum_{s=1}^3 n_s(x, t).$$

For brevity, we denote $n_s = n_s(x, t)$ and $N = N(x, t)$, and $N^{(i,j)}$ denotes the derivatives in space and time according to the notation

$$N^{(i,j)} = \frac{\partial^{i+j}}{\partial^i x \partial^j t} N.$$

In order to be able to define the solution of the PDE system we also need to define initial condition.

In principle, the initial condition in each state can be any function $n_s(x, 0) = f_s(x)$, where $f_s \geq 0$. However, since we assume we can only observe the total particle density, only the total density at time $t = 0$ is known, $N(x, 0) = f(x) = \sum_s f_s(x)$, which gives limited information on the initial condition in each state. In order to be able to study the impact of the initial condition on the solution of the PDE system and its structural identifiability properties, we assume that the initial density in each state s is some proportion of the total initial density, with weight $a_s \geq 0$, for $s = 1, 2, 3$, such that $\sum_s a_s = 1$. Hence, we write the initial condition in each state $s = 1, 2, 3$ as

$$n_s(x, 0) = a_s f(x), \tag{S4}$$

where $f(x) \geq 0$ is measured since $f(x) = N(x, 0)$, and is periodic in $[-L, L]$. We observe that the stationary distribution weights of the stochastic individual-based model give the weights of the homogeneous steady state of the equivalent PDE system.

To showcase examples of model solutions, we consider the case of a far-field initial condition, concentrated around $x = 0$, for a time $t \in [0, 0.5]$. We define an interval $[-L, L]$ where $L > 0$ is large enough compared to $t \max_s |v_s|$, so that the behaviour at the boundary of the domain does not significantly impact the observed numerical solutions. Then, for simplicity of the numerical solutions, we take the boundary conditions to be periodic in the domain $[-L, L]$ for some $L > 0$; hence $n_s(-L, t) = n_s(L, t)$ for all $t \geq 0$. We define the initial condition $f(x)$ as the Gaussian distribution in the interval $[-L, L]$ and we extend it by periodicity to \mathbb{R} , with zero mean and variance $\varsigma^2/2$

$$f(x) = \frac{1}{\sqrt{\pi\varsigma^2}} \exp\left(-\frac{x^2}{\varsigma^2}\right), \tag{S5}$$

with $\varsigma = 5$, and $L = 40$. We note that $f(x)$ is symmetric and $f(L) = f(-L)$.

S3 Structural identifiability measuring single-particle trajectories if two or three states share the same velocity

In this section, we analyse the structural identifiability properties of three-state models in which two or three states share the same velocity.

If all states v_1, v_2, v_3 share the same velocity, v , the particle will move at constant velocity v . Hence, the trajectory will be $x(t) = vt$ for all $t \geq 0$. We note that this type of trajectory can be obtained for models with all velocities equal v , with any switching rates λ_s and any network probability matrix \mathbb{P} . Therefore, only v is identifiable and two individual-based model are equivalent for arbitrarily chosen rates and probability parameters.

Otherwise, without loss of generality, we assume $v_1 \neq v_2 = v_3 = v$. By analysing the distribution obtained from the time spent in each segment with constant

$$\frac{dx(t)}{dt} = v_1,$$

we can directly obtain λ_1 . Moreover, the survival distribution of the total times spent with velocity v , now denoted τ_{23} , is obtained by solving the following recurrence

$$\tau_{23}(t) = p_{12}R_2(t) + p_{13}R_3(t),$$

where the time starting in state $s = 2$ can be expressed as

$$R_2 = \exp(-\lambda_2 t)(p_{21} + p_{23} \exp(-\lambda_3 t)(p_{31} + p_{32}R_2)),$$

and, similarly, the time starting in state $s = 3$ can be expressed as

$$R_3 = \exp(-\lambda_3 t)(p_{31} + p_{32} \exp(-\lambda_2 t)(p_{21} + p_{23}R_3)).$$

The recurrences can be solved to obtain

$$\tau_{23}(t) = \frac{A \exp(-\lambda_2 t) + B \exp(-\lambda_3 t) + C \exp(-(\lambda_2 + \lambda_3)t)}{1 - D \exp(-(\lambda_2 + \lambda_3)t)},$$

where

$$A = p_{12}p_{21},$$

$$B = p_{13}p_{31} = (1 - p_{12})p_{31},$$

$$C = p_{12}p_{23}p_{31} + p_{13}p_{32}p_{21} = p_{12}(1 - p_{21})p_{31} + (1 - p_{12})(1 - p_{31})p_{21},$$

$$D = p_{23}p_{32} = (1 - p_{21})(1 - p_{31}).$$

We note that $A, B, C, D \geq 0$, and, if $\lambda_2, \lambda_3, A, B, C, D$ are identifiable then all model parameters are identifiable as $p_{31} = B/(B + D)$, then $p_{21} = 1 - D/(1 - p_{31})$, and then $p_{12} = A/p_{21}$.

We note that, taking the limit as $t \rightarrow \infty$, the denominator of τ_{23} can be expanded as a geometric series as follows

$$\frac{1}{1 - D \exp(-(\lambda_2 + \lambda_3)t)} = \sum_{k=0}^{\infty} D^k \exp(-k(\lambda_2 + \lambda_3)t),$$

and the dominant term is the one with the lowest exponent, obtained for $k = 0$. We also note that in all cases D is identifiable when A, B, C are, since D can be obtained by solving the equation $\tau_{23}(0) = (A + B + C)/(1 - D)$.

If the leading coefficient (either A or B) is non-zero, we observe that

$$\lim_{t \rightarrow \infty} -\frac{1}{t} \log \tau_{23}(t) = \lambda_{\min}.$$

First, we analyse the case in which the two rates λ_2 and λ_3 are distinct. Without loss of generality, we now fix a state labelling, for example, such that $\lambda_{\min} = \lambda_2 < \lambda_3$. In this case, if $A \neq 0$ we find that λ_2 is identifiable. Then, we have

$$\lim_{t \rightarrow \infty} \exp(-\lambda_2 t) \tau_{23}(t) = A,$$

thus, A is also identifiable. Moreover, if $B \neq 0$ we can also identify

$$\lim_{t \rightarrow \infty} -\frac{1}{t} \log (\tau_{23}(t) - A \exp(-\lambda_2 t)) = \lambda_3,$$

and

$$\lim_{t \rightarrow \infty} \exp(\lambda_3 t) (\tau_{23}(t) - A \exp(-\lambda_2 t)) = B.$$

We also note that

$$\lim_{t \rightarrow \infty} -\frac{1}{t} \log (\tau_{23}(t) - A \exp(-\lambda_2 t) - B \exp(-\lambda_3 t)) = \lambda_2 + \lambda_3 > \lambda_3.$$

Finally, we can identify C as

$$\lim_{t \rightarrow \infty} \exp(\lambda_2 t + \lambda_3 t) (\tau_{23}(t) - A \exp(-\lambda_2 t) - B \exp(-\lambda_3 t)) = C.$$

Hence, in this case all model parameters are identifiable.

If $A = 0$, if $B \neq 0$ we would obtain

$$\lim_{t \rightarrow \infty} -\frac{1}{t} \log \tau_{23}(t) = \lambda_3$$

and

$$\lim_{t \rightarrow \infty} \exp(\lambda_3 t) \tau_{23}(t) = B,$$

but then we would obtain

$$\lim_{t \rightarrow \infty} -\frac{1}{t} \log (\tau_{23}(t) - B \exp(-\lambda_3 t)) = 0,$$

which would imply that $A = 0$. Then, if $C \neq 0$ we obtain

$$\lim_{t \rightarrow \infty} -\frac{1}{t} \log (\exp(\lambda_3 t) \tau_{23}(t) - B) = \lambda_2,$$

and

$$\lim_{t \rightarrow \infty} \exp(\lambda_2 t) (\tau_{23}(t) - B \exp(-\lambda_3 t)) = C.$$

Otherwise, if $C = 0$, then we obtain

$$\lim_{t \rightarrow \infty} -\frac{1}{t} \log (\exp(\lambda_3 t) \tau_{23}(t) - B) = \lambda_2 + \lambda_3 > \lambda_3 > \lambda_2.$$

Hence, λ_2 is identifiable by subtracting λ_3 from their sum and it follows that $C = 0$.

If $A = B = 0$, we are in the cases of a circularly-oriented network, as either $p_{13} = p_{21} = 0$ or $p_{12} = p_{31} = 0$ (since we assume the network cannot be disconnected), which correspond to either switching from state $s = 1$ to state $s = 2$, then to state $s = 3$ and then back to state $s = 1$, or the opposite circular orientation, and

$$\tau_{23}(t) = \frac{C \exp(-(\lambda_2 + \lambda_3)t)}{1 - D \exp(-(\lambda_2 + \lambda_3)t)}.$$

These correspond to the limit case in which

$$\lim_{t \rightarrow \infty} -\frac{1}{t} \log \tau_{23}(t) = \lambda_2 + \lambda_3,$$

and

$$\lim_{t \rightarrow \infty} \exp(\lambda_2 + \lambda_3) \tau_{23}(t) = C,$$

which show that only the sum $\lambda_2 + \lambda_3$ is identifiable, but not λ_2, λ_3 . The two cases, $p_{21} = p_{13} = 0$ versus $p_{12} = p_{31} = 0$, are interchangeable without loss of generality. Moreover, $C = p_{31}$ or $C = p_{21}$, respectively, which implies $C \neq 0$, as otherwise state $s = 1$ would never be visited after the other two states, contradicting the assumption that the Markov chain describing the state evolution is recurrent.

Finally, we need to consider the case in which $\lambda_2 = \lambda_3 = \lambda$, and we have

$$\tau_{23}(t) = \frac{(A + B) \exp(-\lambda t) + C \exp(-2\lambda t)}{1 - D \exp(-2\lambda t)}.$$

If $A = B = 0$, as before, we can only identify the sum $\lambda_2 + \lambda_3$ and there are two equivalent cases. Otherwise, we have $A + B \neq 0$, and we can obtain

$$\lim_{t \rightarrow \infty} -\frac{1}{t} \log \tau_{23}(t) = \lambda,$$

and

$$\lim_{t \rightarrow \infty} \exp(\lambda t) \tau_{23}(t) = A + B.$$

Moreover, if $C \neq 0$, we obtain

$$\lim_{t \rightarrow \infty} -\frac{1}{t} \log(\tau_{23}(t) - (A + B) \exp(-\lambda t)) = 2\lambda,$$

and

$$\lim_{t \rightarrow \infty} \exp(2\lambda t) (\tau_{23}(t) - (A + B) \exp(-\lambda t)) = C.$$

We note that

$$\lim_{t \rightarrow \infty} -\frac{1}{t} \log((\tau_{23}(t) - (A + B) \exp(-\lambda t) - C \exp(-2\lambda t))) = \lambda,$$

and, as $\lambda < 2\lambda < 3\lambda$, the equation highlights that this is a distinct case compared to when $\lambda_2 \neq \lambda_3$ and it allows to identify $\lambda_2 = \lambda_3$. Moreover, D can be identified by solving

$$\tau_{23}(0) = \frac{(A+B)+C}{1-D}.$$

To conclude, we note that

$$p_{21} = 1 - D/(1 - p_{31}),$$

and $p_{12}(1 - D/(1 - p_{31})) + (1 - p_{12})p_{31} = (A + B)$, which gives

$$p_{12} = \frac{(A+B) - p_{31}}{(1 - p_{31})^2 - D}(1 - p_{31}),$$

and we obtain that

$$C = -(A+B) + 1 - p_{31} - D,$$

which implies that p_{12}, p_{21}, p_{31} are all identifiable.

If $C = 0$, then we are in the case $p_{21} = 1$ and $p_{31} = 1$, thus, the states with equal velocity $s = 2$ and $s = 3$ are only connected through state $s = 1$. We can compute

$$\lim_{t \rightarrow \infty} -\frac{1}{t} \log(\tau_{23}(t) - (A+B)\exp(-\lambda t)) = 3\lambda,$$

and we obtain

$$\lim_{t \rightarrow \infty} \exp(2\lambda t)(\tau_{23}(t) - (A+B)\exp(-\lambda t)) = 0 = C.$$

Hence, if $\lambda_2 = \lambda_3$ there is non-identifiability as $s = 2$ and $s = 3$ can be considered a copy of the same state, also referred to as two redundant states. Even assuming that we know there are three states, we cannot distinguish if there are two copies of the state with velocity v_1 or with velocity v_2 .

In summary, the three-state model is structurally identifiable using a single-particle trajectory in which each state has distinct velocity (up to state relabelling). Moreover, it is also identifiable when exactly two states share the same velocity but are not redundant, except for the case of a circularly-oriented network for which only the sum of the rates associated with the same velocity can be identified, but not the individual rates.

S4 Structural identifiability measuring the total particle density if two or three states share the same velocity

In this section, we study the structural identifiability of the process measuring the total particle density, when two or all three states share the same velocity.

If all three states share the same velocity $v_1 = v_2 = v_3 = v$, the differential algebra approach simply gives

$$\frac{\partial N}{\partial t} + v \frac{\partial N}{\partial x} = 0.$$

Indeed, from an initial density $N(x, 0) = f(x)$ we obtain the behaviour the solution of the total density $N(x, t) = f(x - vt)$. Without further assumptions we can only identify the velocity v , but all rate and probability parameters are non-identifiable.

Otherwise, if two states share the same velocity, without loss of generality assume $v_1 \neq v_2 = v_3 = v$, the differential algebra steps to obtain the input-output equation are still valid, and the coefficients obtained can be rewritten as

$$\begin{aligned} \hat{c}_1 &= v_1 + 2v, & \hat{c}_2 &= 2v_1v + v^2, & \hat{c}_3 &= v_1v^2, \\ \hat{c}_4 &= \lambda_1 + (\lambda_2 + \lambda_3), & \hat{c}_5 &= 2\lambda_1v + (\lambda_2 + \lambda_3)(v_1 + v), \\ \hat{c}_6 &= \lambda_1v^2 + (\lambda_2 + \lambda_3)v_1v, \\ \hat{c}_7 &= \lambda_2\lambda_3(1 - (1 - p_{21})(1 - p_{31})) + \lambda_1[\lambda_3(1 - (1 - p_{12})p_{31}) + \lambda_2(1 - p_{12}p_{21})], \\ \hat{c}_8 &= \lambda_2\lambda_3(1 - (1 - p_{21})(1 - p_{31}))v_1 + \lambda_1[\lambda_3(1 - (1 - p_{12})p_{31}) + \lambda_2(1 - p_{12}p_{21})]v. \end{aligned} \tag{S6}$$

The identifiability up to state relabelling of the velocities still holds. The coefficients \hat{c}_4, \hat{c}_5 give identifiability of the rate λ_1 and of the sum $\lambda_2 + \lambda_3$, as $v \neq v_1$, and the coefficient \hat{c}_6 is redundant. Then, the remaining coefficients \hat{c}_7, \hat{c}_8 , simplified for known quantities, together with $\lambda_2 + \lambda_3$, give that the identifiable parameter combinations are

$$k_1 = \lambda_2 + \lambda_3, \quad k_2 = \lambda_2\lambda_3(p_{21} + p_{31} - p_{21}p_{31}), \quad k_3 = \lambda_2p_{12}p_{21} + \lambda_3p_{31}(1 - p_{12}). \tag{S7}$$

We note that k_1, k_2, k_3 do not allow us to identify the parameters $\lambda_2, \lambda_3, p_{12}, p_{21}, p_{31}$. In Section S7 we conclude the study of the structural identifiability of the model with two equal velocities by considering the initial condition.

S5 Examples of equivalent model parametrisations and the impact of the initial condition with velocities all distinct

In this section, we study how the initial conditions of the type $n_s(x, 0) = a_s f(x)$ impact the structural identifiability of the three-state PDE model, by comparing the total density evolutions obtained for models with the same coefficients c_1, c_2, \dots, c_9 .

Now, we showcase examples of models with the same input-output coefficients c_1, \dots, c_8 but different probability parameters p_{12}, p_{21}, p_{31} (Figure S1). First, without loss of generality, we define a parametrised model A. Then, we show the intersection of the quadratic equations given by coefficients c_7 and c_8 , and we choose models B and C with same coefficients as model A. In particular, model B is the only parametrised model to also have the same stationary distribution as model A, respectively, while model C is chosen to have $p_{12} = 0$. These examples are also used to analyse the impact of the initial condition on the total density evolution and, therefore, on their structural identifiability properties.

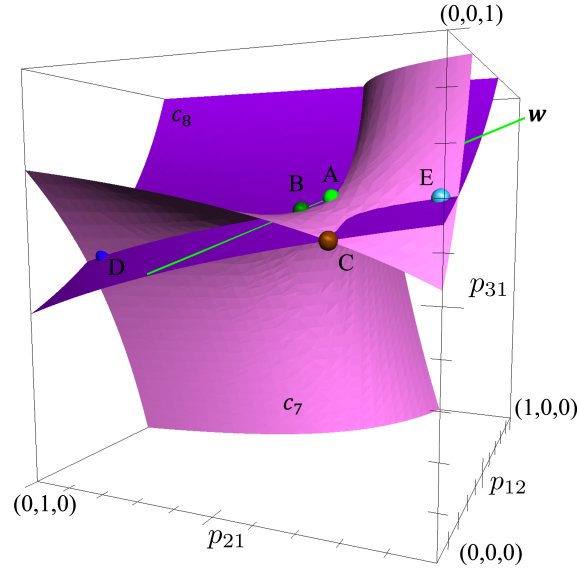


Fig. S1 Example surfaces obtained fixing the coefficients c_7 and c_8 . The surfaces shown are obtained fixing the coefficients $c_7 = 1441/2000$ (pink) and $c_8 = 39/100$ (violet), obtained from model A, assuming identified parameters $\theta = \{v_1 = 20, v_2 = -15, v_3 = 0, \lambda_1 = 1, \lambda_2 = 1/2, \lambda_3 = 3/10\}$ and varying $(p_{12}, p_{21}, p_{31}) \in [0, 1] \times [0, 1] \times [0, 1]$. The graph also shows the points related to the parameters of example models A (light green), B (dark green), C (brown), D (blue) and E (light blue) (further analysed in the Supplementary Information Section S3). The line was obtained fixing the initial condition to be at the stationary distribution $a = w$ (light green). This image was created using Apple Grapher (macOS).

Parametrised models A, B and C

Parametrised models A, B and C are chosen to have switching rates and velocities all distinct. The parameters in common are

$$\boldsymbol{\theta} = \{v_1 = 20, v_2 = -15, v_3 = 0, \lambda_1 = 1, \lambda_2 = 1/2, \lambda_3 = 3/10\}.$$

Without loss of generality, the probability parameters for model A are chosen as follows

$$\boldsymbol{\theta}_A = \boldsymbol{\theta} \cup \{p_{12} = 1/5, p_{21} = 3/10, p_{31} = 7/10\}.$$

The parameters of the three-state models with the same coefficients c_1, \dots, c_8 as $\boldsymbol{\theta}_A$ must lie in the intersection of the surfaces obtained by fixing the coefficients c_7 and c_8 , given by

$$\begin{cases} \frac{1441}{2000} = \frac{3}{20}(1 - (1 - p_{21})(1 - p_{31})) + \frac{3}{10}(1 - (1 - p_{12})p_{31}) + \frac{1}{2}(1 - p_{12}p_{21}), \\ \frac{39}{100} = 3(1 - (1 - p_{21})(1 - p_{31})) - \frac{9}{2}(1 - (1 - p_{12})p_{31}). \end{cases} \quad (\text{S8})$$

We note that there are an infinite number of other sets of probabilities that give the same coefficients in the input-output equation.

Now, model B is chosen to also have the same stationary distribution as model A, and model C is chosen to have $p_{12} = 0$. The parameters for models B and C are chosen as follows

$$\boldsymbol{\theta}_B = \boldsymbol{\theta} \cup \{p_{12} = 66/395, p_{21} = 79/220, p_{31} = 158/235\},$$

$$\boldsymbol{\theta}_C = \boldsymbol{\theta} \cup \{p_{12} = 0, p_{21} = 61/268, p_{31} = 108/175\},$$

and the stationary distribution weights are

$$\boldsymbol{w}_A = \boldsymbol{w}_B = [237/1441, 24/131, 940/1441]^T, \quad \text{and} \quad \boldsymbol{w}_C = [1479/10087, 1608/10087, 1000/1441]^T.$$

In the next section, we study the impact of the initial conditions by comparing numerical solutions for the parametrised models A, B and C for some initial condition weights that fix the coefficient c_9 .

S5.1 Fixing the coefficients c_1, \dots, c_9 is not sufficient to obtain identical total density evolutions

In this section, we obtain numerical solutions for the parametrised models in examples 1 and 2, obtained fixing the coefficients c_1, \dots, c_8 . Moreover, we fix the initial condition weights for model A and for the other models we choose the initial condition weights such that the coefficient c_9 is fixed.

Firstly, we fix the initial condition $\mathbf{a} = [a_1, a_2, 1 - a_1 - a_2]^T$ to be equal to the stationary distribution \mathbf{w} for each model considered. We note that these weights correspond to the initial distribution of the individual-based model in the assumption that the initial measurement could be taken at any point in time. We verify that these weights give the same coefficient c_9 , once the coefficients c_1, \dots, c_8 are fixed. In particular, Figure 3 in the main text shows the intersection between the surfaces obtained from the coefficients c_7 and c_8 and their intersections with the stationary distribution weights \mathbf{w} for model A. We note that the green surface intersects both c_7 and c_8 in their intersection. Thus, if the initial condition weights are equal to the model stationary distribution, all models with the same coefficients c_1, \dots, c_8 initial condition weights are also equal to the model stationary distribution, then c_9 is still fixed.

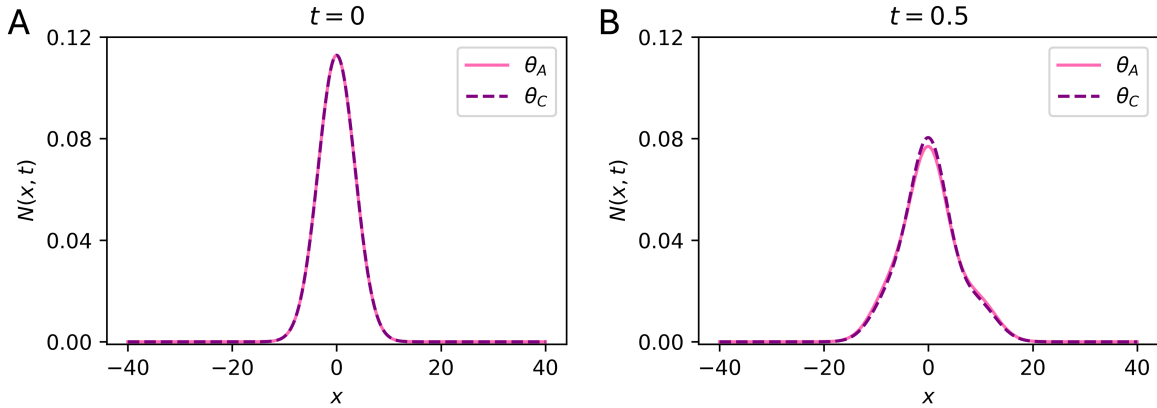


Fig. S2 Numerical solution for the parametrised models A and C with initial condition $\mathbf{a} = \mathbf{w}$ for each model, at times $t = 0$ and $t = 0.5$. The numerical solution for the parametrised model A is compared with the one for model C with $\mathbf{a} = \mathbf{w}$ at times $t = 0$ (panel A) and $t = 0.5$ (panel B). The simulations are obtained with an upwind method, setting the grid to $dx = 0.01$ and $dt = 0.00045$.

We observe that the total density evolution is the same between models A and B (Figure 4), while it is different between models A and C, despite having equal input-output coefficients c_1, \dots, c_9 (Figure S2B), with initial condition $\mathbf{a} = \mathbf{w}$ in each case. Further proof of the significance of the

difference between the total density evolution of these two models is given by comparing their error to an upper bound of the numerical error for the upwind scheme used. Panel **A** in Figure S3 shows errors of an order approximately between 10^{-10} and 10^{-7} for model A versus B, while errors of an order between 10^{-4} and 10^{-2} for model A versus C, which are close to or higher than the upper bound of the numerical error obtained (10^{-4}). Hence, for $\mathbf{a} = \mathbf{w}$, the same initial conditions lead to the same density evolution but different initial conditions do not, suggesting that there is more information on the initial condition weights or on the model parameters than the ones obtained fixing the coefficients c_1, \dots, c_9 .

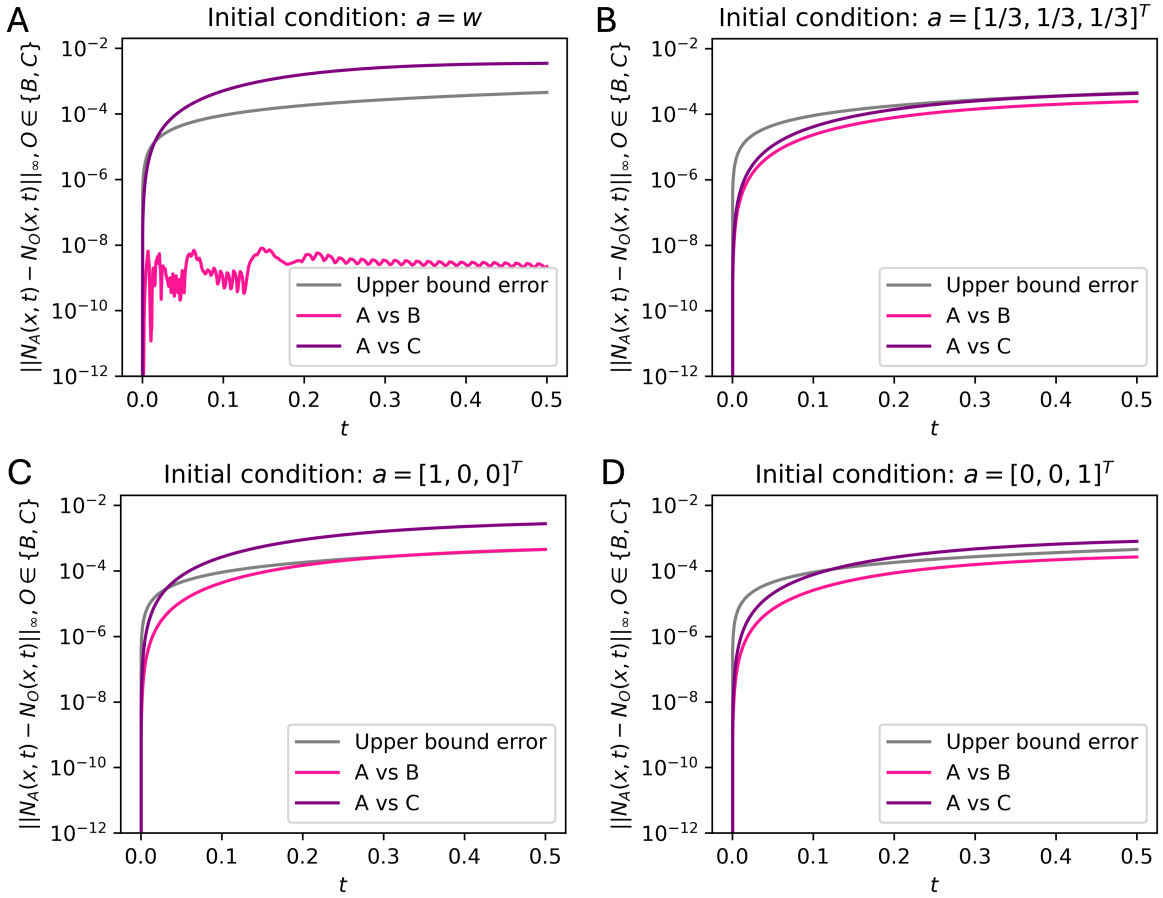


Fig. S3 L-infinity norm of the difference of $N(x, T)$ for model A versus models B and C, as a function of time $t \in [0, T]$, where $T = 0.5$. L-infinity norm of the difference of $N(x, T)$ between model A and models B and C with initial condition weights $\mathbf{a} = \mathbf{w}$ (**A**), $\mathbf{a} = [1/3, 1/3, 1/3]^T$ (**B**), $\mathbf{a} = [1, 0, 0]^T$ (**C**) and $\mathbf{a} = [0, 0, 1]^T$ (**D**).

To further analyse the behaviour of the models solutions, we repeat the same analysis with initial condition equal weights or weights $\mathbf{a} = [1, 0, 0]^T$ and $\mathbf{a} = [0, 0, 1]^T$. In the latter two cases, the choices

of initial conditions corresponds to assuming that all particles at time $t = 0$ are in state $s = 1$, with velocity $v_1 = 20$, or are in state $s = 3$, with velocity $v_3 = 0$, respectively. Figure S3B-D compares the evolution of the error difference of total density $N(x, t)$, for models A to B and C, with initial weights $\mathbf{a} = [1/3, 1/3, 1/3]^T$, $\mathbf{a} = [1, 0, 0]^T$, and $\mathbf{a} = [0, 0, 1]^T$. In each of these cases, we observe that, despite choosing the initial condition weights to be equal across models, the error between the total density evolutions is still large (around 10^{-4} or higher).

Finally, we study how error difference varies with the grid choice, varying dx , for four types of initial conditions, with weights equal to the stationary weights \mathbf{w} , with equal weights $\mathbf{a} = [1/3, 1/3, 1/3]^T$, and with weights $\mathbf{a} = [1, 0, 0]^T$ and $\mathbf{a} = [0, 0, 1]^T$ corresponding to all the initial density being in the state with velocity $v_1 = 20$ or $v_3 = 0$, respectively. In Figure S4 we show the L-infinity norm of the difference of the total density evolution between models in examples 1 and 2 at time $T = 0.5$, and we interpret the norms close to or above the upper bound error to be significant, and the significantly lower values to be numerical artefacts.

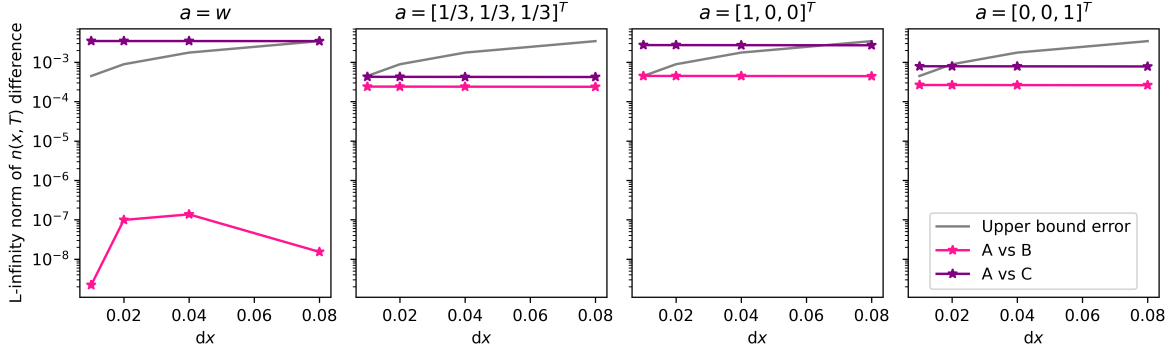


Fig. S4 L-infinity norm of the difference of $N(x, T)$ between model A and models B and C at $T = 0.5$. The L-infinity norms of $N(x, T|\theta_A) - N(x, T|\theta_B)$ (pink), $N(x, T|\theta_A) - N(x, T|\theta_C)$ (purple) are shown. The x grid increment dx is varied in the set $\{0.01, 0.02, 0.04, 0.08\}$, and the dt is also varied to guarantee numerical stability of the PDE solver. The grey line represents an upper bound for the numerical error as the grid is varied.

Overall, these results suggest that there may be additional parameter combination coefficients related to the initial condition weights and to the other model parameters that also need to be conserved to make the evolution of equivalent models the same. In the next section, we obtain the PDE model characteristics, on which the system PDEs can be reduced to ODEs, and use these ODEs to find additional coefficients that relate to the model parameters and initial conditions.

In the next section, we analyse the impact of the coefficients c_{10}, \dots, c_{15} obtained in Section 4.2 (main text) using this method on the model identifiability.

S5.2 The coefficients c_1, \dots, c_{15} give local structural identifiability

In this section, we analyse the impact of the coefficients c_{10}, \dots, c_{15} (Section 4.2, main text). We note that, for velocities all distinct and initial conditions specified in Equation (S4), all model parameters including the initial condition weights become locally structurally identifiable by fixing all coefficients c_1, \dots, c_{15} . In particular, all parameters are globally structurally identifiable except the three probability parameters which are always at least locally identifiable.

We already showed an example of this local identifiability. Indeed, models A and B, with weights $\mathbf{a} = \mathbf{w}$, have the same total particle density evolution (Figure S2 left panels, and Figure S3A). However, depending on the initial conditions there are other examples sharing the same total density evolution.

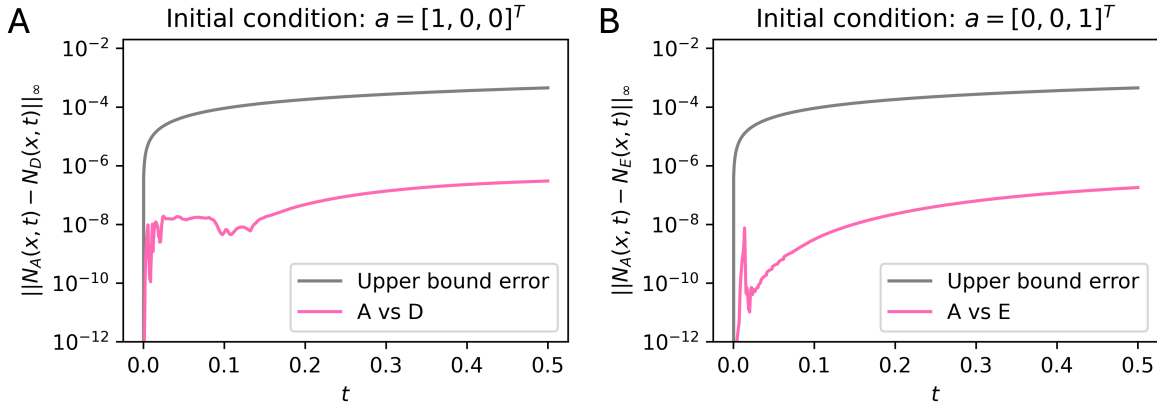


Fig. S5 L-infinity norm of the difference of $N(x, T)$ between model A and model D and E as a function of time $t \in [0, T]$, where $T = 0.5$. **A** L-infinity norm of the difference of $N(x, T)$ between model A and model D with initial condition weights $\mathbf{a} = [1, 0, 0]^T$. **B** L-infinity norm of the difference of $N(x, T)$ between model A and model E with initial condition weights $\mathbf{a} = [0, 0, 1]^T$.

For model 1A with $\mathbf{a} = \mathbf{w}$, we find that the only equivalent model is model 1B, while if 1A starts at weights $\mathbf{a} = [1, 0, 0]^T$, or $\mathbf{a} = [0, 0, 1]^T$, there is no structurally equivalent model. For model A with $\mathbf{a} = \mathbf{w}$, we find that the only equivalent model is model B. In contrast, if A starts at weights $\mathbf{a} = [1/3, 1/3, 1/3]^T$ there is no structurally equivalent model, making this parameter set structurally identifiable. For model A with $\mathbf{a} = [1, 0, 0]^T$ there is exactly one equivalent model (Figure S5A), denoted model D, with parameters

$$\boldsymbol{\theta}_D = \boldsymbol{\theta} \cup \{p_{12} = 1/5, p_{21} = 47/50, p_{31} = 23/42\}.$$

For model A with $\mathbf{a} = [0, 0, 1]^T$ there is exactly one equivalent model (Figure S5B), denoted model E, with parameters

$$\boldsymbol{\theta}_E = \boldsymbol{\theta} \cup \{p_{12} = 87/700, p_{21} = 7/200, p_{31} = 7/10\}.$$

S6 There exist three linearly independent vectors of the type $\mathbf{F}_z(t)$ if all three velocities are distinct

Here, we prove that if the velocities are all distinct, for any function $f(x)$ that is not constant there exists a set $Z = \{\zeta_1, \zeta_2, \zeta_3\}$ such that the vectors

$$\mathbf{F}_z(t) = [f(\zeta_z - v_1 t), f(\zeta_z - v_2 t), f(\zeta_z - v_3 t)], \quad (\text{S9})$$

are linearly independent for $z = 1, 2, 3$, for some arbitrarily small $t > 0$. For a fixed $t > 0$ sufficiently small, we can take, for example, $\zeta_1 = v_1 t$, $\zeta_2 = v_2 t$ and $\zeta_3 = v_3 t$, and define

$$\mathbf{F} = \mathbf{F}(t) = \begin{bmatrix} f(0) & f((v_1 - v_2)t) & f((v_1 - v_3)t) \\ f((v_2 - v_1)t) & f(0) & f((v_2 - v_3)t) \\ f((v_3 - v_1)t) & f((v_3 - v_2)t) & f(0) \end{bmatrix}, \quad (\text{S10})$$

and we can denote $\mathbf{F} = [F_{zs}]_{zs}$ where $F_{zs} = f((v_z - v_s)t)$. We can study the identifiability of the coefficients c_{10}, \dots, c_{15} by studying the rank of \mathbf{F} . Indeed, if \mathbf{F} has got full rank, then the coefficients are structurally identifiable.

We note that for $f(x)$ Gaussian, we have

$$F_{zs} = f((v_z - v_s)t) = \frac{1}{\sqrt{\pi\zeta^2}} \exp\left(-\frac{((v_z - v_s)t)^2}{\zeta^2}\right),$$

and \mathbf{F} is symmetric and, for all $t > 0$, $F_{zs} > 0$. We perform row reduction on the matrix \mathbf{F} , which preserves the matrix rank, and we obtain the row-reduced matrix

$$\hat{\mathbf{F}} = \begin{bmatrix} f(0) & f((v_1 - v_2)t) & f((v_1 - v_3)t) \\ 0 & f(0)^2 - f((v_1 - v_2)t)^2 & f(0)f((v_2 - v_3)t) - f((v_1 - v_3)t)f((v_1 - v_2)t) \\ 0 & 0 & f(0)f((v_1 - v_2)t) - f((v_1 - v_3)t)f((v_2 - v_3)t) \end{bmatrix}.$$

We note that $\hat{F}_{11} \neq 0$, as $f(0) > 0$, and $\hat{F}_{22} = f(0)^2 - f((v_1 - v_2)t)^2 \neq 0$, if and only if $v_2 \neq v_1$. Similarly, $f(0)f((v_1 - v_2)t) - f((v_1 - v_3)t)f((v_2 - v_3)t) = 0$ if and only if $(v_1 - v_2)^2 = (v_1 - v_3)^2 + (v_2 - v_3)^2$, if and only if $(v_3 - v_1)(v_3 - v_2) = 0$. Hence, $\hat{F}_{33} \neq 0$ provided that $v_3 \neq v_1, v_2$. In conclusion, if all velocities are distinct the matrix \mathbf{F} has got full rank and the coefficients c_{10}, \dots, c_{15} are all identifiable.

For other forms of $f(x)$ we can generalise the proof. We assume that the generic function $f(x) \in C^2$ has a strict local maximum, and, without loss of generality we can assume that $f(0)$ is the strict local maximum, and $f'(x) = 0$ and $f''(0) < 0$. Using the rule of Sarrus, we write

$$\det(\mathbf{F}) = F_{11}F_{22}F_{33} + F_{12}F_{23}F_{31} + F_{13}F_{21}F_{32} - F_{11}F_{23}F_{32} - F_{12}F_{21}F_{33} - F_{13}F_{22}F_{31}.$$

For $t > 0$ sufficiently small, then also $(v_z - v_s)t \rightarrow 0$, and we can write the Taylor expansion about $x = 0$ as

$$f(x) = f(0) + \frac{f''(0)}{2}x^2 + o(x^2),$$

since $f'(0) = 0$. Hence, we write

$$F_{zs} = f(0) + \frac{f''(0)}{2}(v_z - v_s)^2 t^2 + o(t^2),$$

and, by substitution, we obtain that

$$\det(\mathbf{F}) = \frac{f''(0)^3}{4}(v_1 - v_2)^2(v_2 - v_3)^2(v_3 - v_1)^2 t^6 + o(t^6).$$

Then, since $f''(0) \neq 0$, in the assumption that all velocities are distinct, we have that $\det(\mathbf{F}) > 0$. We conclude that \mathbf{F} has got full rank, and, therefore, the coefficients are structurally identifiable.

S7 Structural identifiability measuring the total particle density if two or three states share the same velocity incorporating the initial condition

In this section, we study the structural identifiability of the process measuring the total particle density, when two or three states share the same velocity, incorporating the initial condition $n_s(x, 0) = a_s f(x)$, $s = 1, 2, 3$. If all three states share the same velocity $v_1 = v_2 = v_3 = v$, we already considered the

initial condition and, in Section S4, we obtained that only v is identifiable, while all other parameters are non-identifiable.

In the case of two states sharing the same velocity, ($v_2 = v_3 = v$), in Section S4 we obtained that the parameters v_1, v, λ_1 are identifiable, and we obtained the additional identifiable parameter combinations k_1, k_2, k_3 . From the differential algebra approach on the initial condition we obtain $N^{(0,1)}(x, 0) + \hat{c}_9 f'(x) = 0$, that gives the identifiable coefficient

$$\hat{c}_9 = a_1(v_1 - v) + v,$$

which allows to identify a_1 .

Moreover, we note that we can still apply the Taylor expansions method to incorporate the initial condition in the structural identifiability analysis. In Section S6, we obtained that there exist $\zeta_1, \zeta_2, \zeta_3$ such that the matrix of the respective vectors $\mathbf{F}_z(t) = [f(\zeta_z - v_1 t), f(\zeta_z - v_2 t), f(\zeta_z - v_3 t)]$ has rank three. In contrast, if $v_2 = v_3$, then the matrix formed by any three vectors $\hat{\mathbf{F}}_z(t) = [f(\zeta_z - v_1 t), f(\zeta_z - vt), f(\zeta_z - vt)]$ has rank as most two as the last two columns are always equal, and it is trivially equal to two if f is not constant for an appropriate choice of ζ_1, ζ_2 .

Hence, we obtain the following additional coefficients

$$\hat{c}_{10} = a_1, \quad \hat{c}_{11} = a_2 + a_3, \quad \hat{c}_{12} = -\lambda_1 a_1 + \lambda_2 p_{21} a_2 + \lambda_3 p_{31} a_3, \quad \hat{c}_{13} = \lambda_1 a_1 - \lambda_2 p_{21} a_2 - \lambda_3 p_{31} a_3.$$

Coefficients $\hat{c}_{10}, \hat{c}_{11}$ do not add any information, as we have already obtained identifiability of a_1 , and, by definition, $a_2 + a_3 = 1 - a_1$. Moreover, we notice that $\hat{c}_{13} = -\hat{c}_{12}$, therefore, the only additional coefficient to consider is \hat{c}_{12} , which, considering the known quantities, can be simplified as the parameter combination

$$k_4 = +a_2 \lambda_2 p_{21} + \lambda_3 p_{31} (1 - a_1 - a_2). \tag{S11}$$

We conclude that the model is non-identifiable as there are four parameter combinations k_1, k_2, k_3, k_4 which cannot be sufficient to identify all six remaining model parameters $\lambda_2, \lambda_3, p_{12}, p_{21}, p_{31}, a_2$.

Declarations

For the purpose of open access, the author has applied a CC BY public copyright licence to any author accepted manuscript arising from this submission.

References

- [1] Ceccarelli, A., Browning, A.P., Chaiamarit, T., Davis, I., Baker, R.E.: A likelihood-based Bayesian inference framework for the calibration of and selection between stochastic velocity-jump models. *Journal of the Royal Society Interface* **23**(236), 20250866 (2026) <https://doi.org/10.1098/rsif.2025.0866>
- [2] Ceccarelli, A., Browning, A.P., Baker, R.E.: Approximate solutions of a general stochastic velocity-jump model subject to discrete-time noisy observations. *Bulletin of Mathematical Biology* **87**(57) (2025) <https://doi.org/10.1007/s11538-025-01437-x>